UNIVERSITÀ DI PARMA

UNIVERSITA' DEGLI STUDI DI PARMA

PhD in Biotechnology and Life Science

XXXII CICLE

Reliable Molecular Markers to Assess the Potential Genotoxicity of Metal Based ENM in Plants

Coordinator:
Prof. Simone Ottonello

Tutor:
Prof. Marta Marmiroli

PhD Candidate: Jacopo Magnani

Academic Years 2016/2019

SUMMARY

1. INTRODUCTION

1.1. GENERALITIES ON NANOMATERIALS

1.1.1. Definition of Nanomaterial

One of more exhaustive definitions of nanomaterial (NM) now available is the 2011 EU definition (*Recommendation on the definition of nanomaterial (2011/696/EU)*).

In this document, a NM is defined as:

"*a natural, incidental or manufactured material containing particles, in an unbound state or as an aggregate or as an agglomerate and where, for 50% or more of the particles in the number size distribution, one or more external dimensions in the size range 1-100 nm.*

In specific cases and where warranted by concerns of the environment, health, safety or competitiveness the number size distribution threshold of 50% may be replaced by a threshold between 1 and 50%.

By derogation from the above, fullerenes, grapheme flakes and single wall carbon nanotubes with one or more external dimensions below 1 nm should 'be considered as nanomaterials." (ec.europa.eu).

1.1.2. Nanomaterial Typologies

The EU classifies the NM also on the base of their origin (natural, incidental or manufactured/intentionally produced). However, for the aims of this work, we consider particularly the intentionally produced NM called engineered nanomaterials or ENM (Fig. 1.1.).

One effective way for classifying ENM is the EPA classification based principally on their chemical properties (EPA, 2007). In general, the classification of ENM based on chemical properties is the most accepted and used (Martínez-Fernández *et al*. 2017).

According to EPA, ENM are classifiable in four principals types:

- Carbon based ENM (composed mostly of carbon and used to create strong and light covers for example in electronics):
    - Fullerenes (spherical or ellipsoidal);
    - Nanotubes (cylindrical);
    - Graphene (one atom layer);
- Metal based ENM:
    - Quantum dots (QDs are closely packed semiconductor crystals comprised by hundred or thousand atoms);
    - Nanogold;
    - Nanosilver;
    - Metal oxides:
        - ZnO NM;
        - CeO_2 NM;
        - TiO_2 NM;
        - *n*FeO_x NM;
        - CuO NM;
        - Ag Based NM;
- Dendrimers (nanosized polymers built from branched units that terminate with numerous chain ends; they find application as drug deliverer);
- Composites (combined ENM with other ENM or with larger, bulk-type materials).

Fig. 1.1. Graphical representations of some ENM types on the base of their structure (researchpower2.ewha.ac.kr).

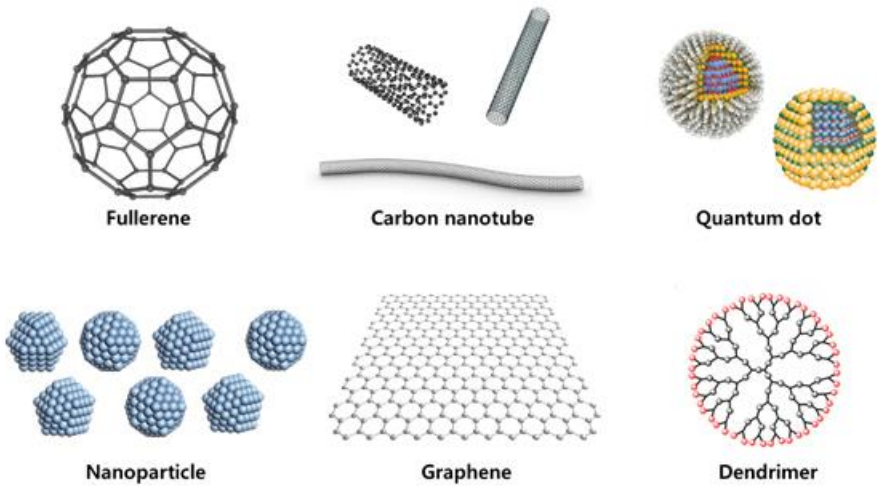

1.1.3. Applications

Exploiting bottom-up (self-assembling) or top-down (milling) processes acting on basic constituents, ENM are produced, by nanotechnology, to exhibit novel characteristics (*e.g.* particular mechanical, catalytic, magnetic, thermal properties, chemical reactivity/conductivity) compared with the same material without nanometric scale features (called bulk substances) (EPA, 2007; www.epa.org). Furthermore, the same ENM may have different nanoforms that differ by size, shape of the constituent particles, surface modification or surface treatment (euon.echa.europa.eu).

Thanks to their peculiar and useful features, ENMs already constitute a billion dollars market (ec.uropa.eu). As a fact, ENMs already find applications in sectors such as public health, employment and occupational safety and health, industry, innovation, environment, energy, transport, security and space, and it's possible to find them in many common products like paints, drugs, cosmetics or batteries (ec.europa.eu; echa.europa.eu; euon.echa.europa.eu).

In this work has been tested two different type of ENMs, metal based quantum dots (QDs) and metal based nanoparticles. QDs find application in fields like cancer research (allow to obtain images as contrast medium), in computer technology (as components of displays) and communication services (miniature lasers to high speed data transfer), solar systems (understandingnano.com).

Metal based nanoparticles find application in cancer medicine (targeting tumours), infections cure (breaking aggregates of bacterial cells, *e.g.* Fe based NPs), antioxidants effects (Ce based NPs allow to remove oxygen free radicals from patient's blood), pollutants removal from water, solar systems (understandingnano.com).

1.2. HEALTH AND ENVIRONMENTAL RISK

To date, there is still a strong scientific uncertainty about the safety of ENM because their heterogeneity and behaviour if compared with the respective bulk substances or compounds with the same chemical composition. For this reason, it becomes difficult to make general statements about ENM safety (eoun.echa.europa.eu).

In general, ENM aren't intrinsically hazardous for human health or environment *per se,* but there may a need to take into account specific consideration in their risk assessment. Only the results of a proper risk assessment (done on a case-by-case basis) that will determine whether an ENM is hazardous and whether or not further action is justified (ec.europa.eu).

There is always the possibility that some ENM could potentially represent a risk for both human and environment health. In fact, because of their widespread use, consumers, workers, and the environment may be exposed to ENM in many different ways (EPA, 2007; euon.echa.europa.eu).

The potential risk derives principally (but not only) from the peculiar physical and chemical features of ENM, and from persistency, although many researches are trying to develop easy and safely degradable ENM (EPA, 2007).

In order to avoid some NMs potential negative effects, several procedures/frameworks of risk assessment are being developed and compared (Oomen *et al*., 2017).

In general, the product of a risk assessment is a statement regarding the probability that humans (populations or individuals) or other environmental receptors, exposed to NM, will be harmed and to what degree this can happen (EPA, 2007).

Although there are different risk assessment procedures, all of these present the same steps (schematic represented in Fig. 1.2.):

- Hazard identification;
- Dose/response assessment;
- Exposure assessment;
- Risk characterization.

Since the aim of this work is to assess the potential genotoxic effect of several metal based NMs on the model plant *Arabidopsis thaliana*, afterwards in this chapter, will be considered principally the genotoxic effects on plants for the principal types of metal based NM reported in scientific literature. For each NM, the most important morphological and physiological effects will be mentioned.

Fig. 1.2. Schematic representation of a risk assessment procedure performed on nanomaterials (Hristozov *et al.*, 2016).

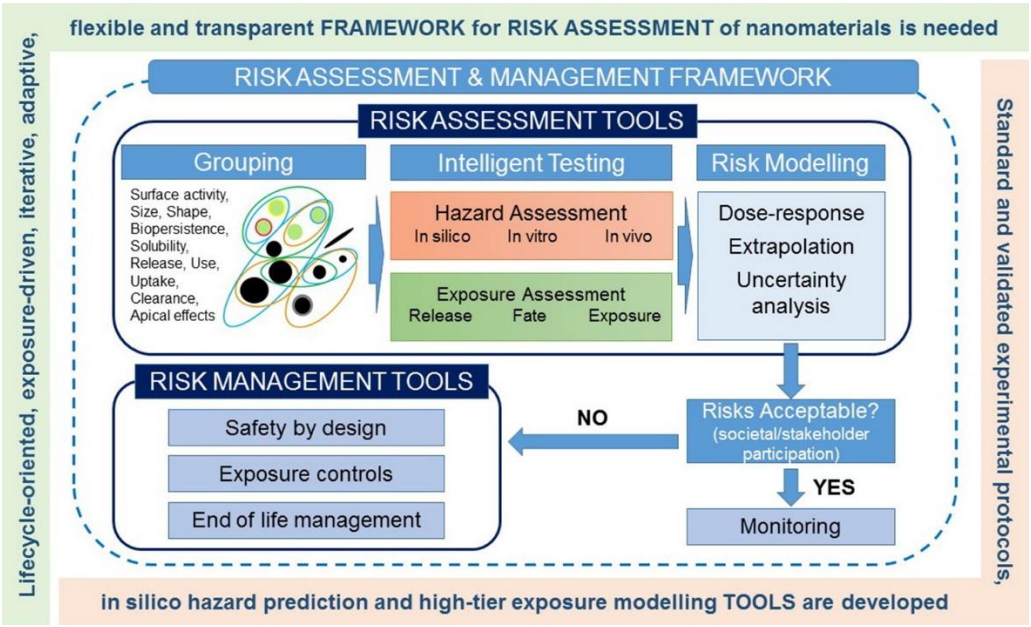

1.2.1. ***Human Health Risk***

It Has been confirmed by several studies that some NM have the ability, due to their peculiar features, to pass easily trough animal cell membranes and potentially being carried through the blood-brain barrier. For example, inhaled NM could be lodged in lungs or be carried by blood in other tissues (EPA, 2007). After arriving in a specific site, NM may have some deleterious effects.

One of the most important possible deleterious effects of NM on living organisms is the genotoxic or mutagenic effect.

There are two principal types of genotoxic effects (Doak *et al*., 2017):

- Small lesions at very specific DNA sites (*e.g.* DNA adducts, DNA cross-links, abasic sites, point mutations);
- Gross abnormalities at chromosome level (*e.g.* aneuploidy, clastogenicity, chromosomal rearrangement).

The genotoxic effects are important since they're often in relation with the formation of cancer cells. Carcinogenesis is a process that results in an accumulation of multiple genome-wide mutations that transforms normal cells into premalignant foci, as demonstrated in many studies in model animals and human cells cultures (Demir *et al*., 2017; Doak *et al*., 2017).

As clearly descript by Doak *et al*. (2017), there are two possible mechanisms, for NM, to induce genotoxic effects:

- Primary mechanism: imparted by NMs themselves (chemically or physically), at the level of a single cell, directly on DNA or indirectly by interaction with other biomolecules involved in the cell division process;
- Secondary mechanism: refers to the ability of NMs to induce a (chronic) inflammatory response by excessive generation of reactive oxygen species (ROS) by macrophage and neutrophil cells at the exposure site. In this case, anti-inflammatory process fails due to the persistence of NMs in exposure site.

It was demonstrated by several (but still limited) studies that both carbon-based NM (fullerenes or C_{60}, carbon nanotubes, graphene, carbon black and carbon diamonds) and metal-based NMs (metal-based QDs, metal-based NPs and metal oxides) are responsible, in many cases, of carcinogenesis in humans (Doak *et al*. (2017).

Anyway, in the majority of these studies, the principal causes of genotoxicity are, in general, reactive oxygen species (ROS). ROS are responsible for inducing

toxicity creating damage to biomolecules (lipids, proteins and nucleic acids) then to cellular structures (*e.g.* cell membranes), or by modulation of antioxidant defence system components and cellular redox homeostasis (Martínez-Fernández *et al*. 2017).

1.2.2. Environmental Risk

Nowadays it can be considered a proven fact that NM have a great potential to improve the environment quality, both through direct (*e.g.* in pollutants remediation and phytoremediation of both soils and waters, environmental engineering) and indirect applications (as constituent of sustainable technologies such as sensors) (EPA, 2007; Martínez-Fernández *et al*. 2017).

Nevertheless, since the environmental quality is strictly in relation with human health, the potential risk of NMs on natural environment, ecological populations and communities must be assessed with attention (EPA, 2007; Holden *et al*., 2013).

Unfortunately, as pointed by EPA (2007), Lowry *et al*. (2012), Gardea-Torresdey *et al*., (2014), and Holden *et al*. (2017), the actual impacts of NM on environmental systems isn't exhaustively documented and understood.

One of the principal difficulties, in assessing environmental risk, is to create experimental conditions that reproduce, with fidelity, the complexity of a real environment, and to standardize eco-toxicological protocols for NM showing completely different behaviour (Gardea-Torresdey *et al*., 2014; Selke *et al*., 2016; Holden *et al*., 2017; Oomen *et al*., 2017).

Other difficulties arise in direct detection of the presence of NMs in the environment since the presence of natural NMs (*e.g.* combustions particulate) disturbs the analysis (EPA, 2007).

General advises on the ecotoxicological test to perform on NMs are given by EPA (2007) regarding the animal or plant species to prefer and the experimental conditions. For example, the species that result more sensitive in laboratory tests must be preferred since they can be used as bioindicators in the external environment. Importantly, as today, the species used in laboratory ecotoxicological tests on NM are the same used in classical ecotoxicological tests.

In general, animal species (*e.g. Daphnia magna*, *Mus musculus*, *Danio rerio*), must be preferred in testing the potential capacity of NM to enter across endothelium, epithelium, lungs, gills etc. while plant species (*e.g. Zea mays*, *Glycine max*) could represent models to assess the potential quantity of NMs that enter in the food chain. Long term studies (or chronic studies) must be preferred and possibly conduct in mesocosms or, when possible, directly in field (EPA, 2007; Holden *et al*., 2016).

Once released, incidentally or voluntarily, NM could remain in one of the three principal environmental matrices: air, soil or water.

Martínez-Fernández *et al*. (2017) report that only in 2010 the global production of NM was estimated to be 260000-390000 metric tons; of which about 8-28, 0.4-7 and 0.1-1.5% were estimated to have ended up in the soil, water bodies and atmosphere respectively.

The fate of NM is principally influenced by two factors (Ma *et* al., 2015; Martínez-Fernández *et al*. 2017; Selke *et al*. 2016):

- The physico-chemical features of NM (surface/volume ratio, dimension, charge, chemical composition, etc);
- The features of the environment (pH, temperature, water salinity, etc).

For example, the high surface/volume rate and the high reactivity of NM influence their fate, transport, toxicity, bioavailability and bioaccumulation capacity, making them very dynamic in the environmental systems (Holden *et* al., 2013; Lowry *et al*., 2012; Ma *et al*., 2015).

The release of NMs in air could result in the transport (strongly influenced by meteorological condition) for kilometres, and their deposition far away from the origin point. In this way, animal organisms, could potentially inhale the particles.

If released in soil, NMs could interact with clays or humic substances and be trapped in the soil matrix but, in this way, they could potentially become bioavailable (*e.g.* by plants uptake).

Even in water NMs could interact easily with suspended particles and become bioavailable for filter organism or be uptaken by microorganism at the food chain base.

In general, potential transformation processes that may occur to NM in the environment influence their behaviour.

The transformations types, as pointed by Lowry *et al*. (2012), can be classified in three principal categories:

- Chemical (oxidation and reduction reactions)
- Physical (aggregation whit other NM or whit natural particles)
- Biological (redox reactions in intracellular, extracellular or soil matrixes)

All these transformations influence the bio-availability of NMs in different ways. For example, as stated above, the aggregation of some NM particles around organic matter particle could increase the probability of NMs to enter inside the food chain (Lowry *et al*., 2012; Selke *et al*. 2016) while an oxidation process can result in a release of toxic metals ions (EPA, 2007).

Another problem arises when the interactions between NM and pollutants already present in the environment is considered. The interactions with pollutants could significantly reduce, increase or, in general, modify the toxicological and eco-toxicological behaviour of both NM and pollutants (Deng *et al*., 2017; Gardea-Torresdey *et al*., 2014; Selke *et al*., 2016).

However, despite the lack of data, one of the major problems for the environmental systems is the biomagnification process of NM in food chains due to their potential persistence (Gardea-Torresdey *et al*., 2014; Martínez-Fernández *et al*. 2017; Ma *et al*. 2018). In fact, as stated by EPA (2007), many of the NM in current use are composed by non-biodegradable inorganic chemicals. Furthermore, environmental fate processes may be too slow to removal of persistent NMs before they can be taken up by organisms (EPA, 2007).

As reported by Gardea-Torresdey *et al*., (2014), Ma *et al*., (2015) and Ma *et al*. (2018), an increasing number of studies performed in mesocosms conditions highlight how NMs can be subject to trophic transfer along the food chain, and potentially reach humans through food.

Other studies (EPA, 2007; Holden *et al*., 2013) reported as different types of NM can greatly modify the soil microbial activity in terrestrial environments and the phytoplankton community life in aquatic environments compromising the functionality of ecological services.

1.3. REGULATION

1.3.1. E.U. Regulation

The most recent publication concerning with nanomaterial (2018) it's the *Public consultation on the draft EFSA guidance on the risk assessment of the applications of nanonscience and nanotechnologies in the food and feed chain: Part 1, human and animal health*, which propose a tiered approach to exposure assessment and hazard assessment for human and animal health (efsa.europa.eu), although the principal regulatory instruments applied by EU on NM are the *Second Regulatory Review on Nanomaterials* and *The Commission Staff Working Paper* (ec.europa.eu).

Recommendation on the definition of nanomaterial (2011/696/EU) concluded that REACH (the regulation of EU adopted to improve the protection of human health and environment from the risk that can be posed by chemicals) and CLP (*Regulation 1272/2008 on classification, labelling and packaging*) offered the best possible framework for the risk management of NM. However, within these regulations more specific requirements on NM are necessary (ec.europa.eu).

Therefore, it becomes important to notice that, for the EU, NM are covered by the same regulatory framework that ensure the safe use of all chemicals and mixtures, and how NM are defined only on the base of the size of constituent particles, without regard to the hazard or risk (euon.echa.europa.eu).

Working in collaboration with member states of EU, competent authorities, the EU, stakeholders and OECD (*Organization for Economic Cooperation and Development*), the most important entity that provides to enforce the use of NM is ECHA (*European Chemicals Agency*).

ECHA, following REACH and CLP regulations, handles whit registration, evaluation, authorization, restriction, classification and labelling of NM (echa.europa.eu).

1.3.2. U.S. Regulation

In the US, there is no federal or state legislation specific to NM. NM are managed by current regulatory framework for chemicals, pesticides, food, cosmetics and drugs. The main authorities involved are the EPA (*United States Environmental Protection Agency*) and FDA (Food and Drug Administration) (www.chemsafetypro.com).

To ensure that NM are manufactured and used without causing damage to human health and environment, EPA is pursuing a comprehensive regulatory approach under TSCA (*Toxic Substances Control Act*) (www.epa.org).

TSCA (passed by the United States Congress in 1976) is the law that provides EPA with authority to require, record-keeping and testing requirements, and restrictions relating to chemical substances and/or mixtures (www.epa.org). The most recent update regarding NM in TSCA, made in 2015 by EPA, is the proposal of new rules to require reporting and recordkeeping information on certain chemical substances when they are manufactured or processed as nanoscale materials (www.chemsafetypro.com). Importantly, as for E.U. regulations, also U.S. regulation considers NM on a par with common chemical substance without nanoscale features.

FDA (*U.S. Food and Drug Administration*), with the specific FDA Nanotechnology Task Force formed in 2006, provides means to identify and recommend ways to address any knowledge useful to evaluate the potential negative effects of NM on human health and environment (www.fda.org).

1.4. NANOMATERIALS AND PLANTS

1.4.1. Effects on Plants

NM can have harmful effects on plants.

Nanoecotoxicological studies are providing a good understanding as demonstrated by the increasing number of publications. However, many results are contradictory and the safety of NM represents a barrier to their wide use (Martínez-Fernández *et al*. 2017).

As reported by de la Rosa *et al*. (2017) and Tripathi *et al*. (2017), there are four principal types of NM phytotoxic effects on plants:

- morphological/anatomical
- physiological
- biochemical
- genetic

An interesting schema of ENM genotoxicity on plants as been provided by Wang *et al*. (2013), where all hypothesized ways of genotoxicity are represented (Fig. 1.3.).

Fig. 1.3. Schematic representation that highlights how ENM could potentially cause a genetic damage to plants.

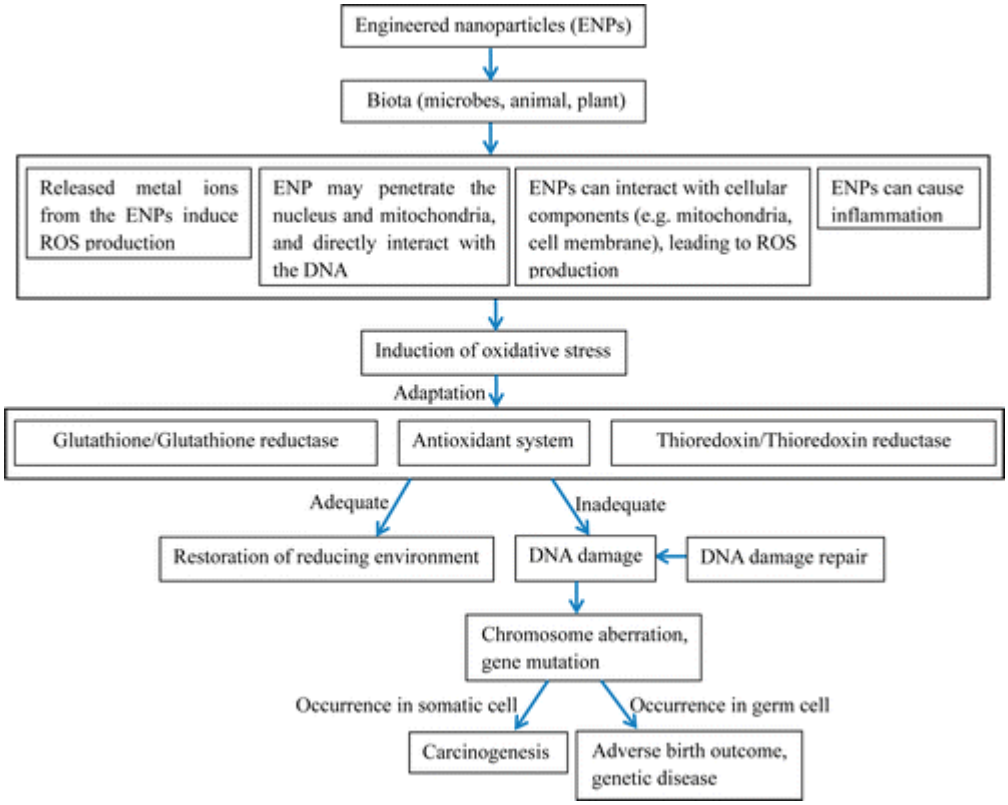

As pointed above (Cap. 2), principally the literature on genotoxic effects on plants was considered in this work, but in each case, the most important physiological and morphological effects are outlined.

In recent literature on the genotoxic effects in plants, is possible to find that the most tested types of ENMs are metal oxide ENMs, such as ZnO NPs (Gosh *et al*., 2016; Priester *et al*., 2017; Zuverza-Mena *et al*., 2017), CeO_2 NPs (Priester *et al*., 2017; Zuverza-Mena *et al*., 2017), Ag-based ENM (Becaro *et al*., 2017), TiO-based ENM (Cox *et al*., 2016).

Other relatively less tested types of ENM on plants are Au, Fe oxides and Cu oxides NM (Reddy *et* al., 2016; Zuverza-Mena *et al*., 2017).

1.4.2. CuO Nanoparticles

Copper oxides NPs genotoxicity has been studied for the first time on some agricultural and grasslands plants by Atha *et al*. (2012). In this study the authors highlight how CuO NPs induce a significant presence of mutagenic lesions, likely

due to the oxidative stress, on three different species of terrestrial plants (*Raphanus sativus*, *Lolium perenne*, and *Lolium rigidum*) under laboratory conditions.

Subsequently, an interesting study conducted on *Fagopyrum esculentum* with a set of 11 RAPDs (*OPA10* included, see § 3.5.) by Lee *et* al., (2013), highlight differences in amplification profiles on roots cells of plants germinated in presence of 4000 mg/L of CuO NPs.

Similar results have been provided by other studies such as Pramanik *et al.* (2017), in which micronuclei test and comet assay performed on roots cell tips of *Coriandrum sativum* were indicative of chromosomal brakeage. This study highlights also the strong production of ROS probably involved in the mutagenic effects.

1.4.3. ZnO Nanoparticles

Zinc oxide (ZnO) NM are generally very unstable, as demonstrated in several studies performed using XAS technique (Ma *et al*., 2015). In fact, XAS allowed to demonstrate how, after exposition, ZnO NM are completely absent in plants tissues but are present high quantity of Zn^{2+} ions. This last feature makes Zn based NM more toxic than other metal based NMs (Ruotolo *et al*., 2018).

In *A. thaliana*, for example, concentrations ranging between 4-100 ng/L of ZnO NM produces negative effects on growth and morphology, as well as oxidative stress, problems in roots development, protein synthesis and energetic balance. These effects are similar to those observed in plants exposed to Zn^{2+} ions. Other effects include overexpression of genes involved in N and P accumulation, modification of lateral roots formation, increase of roots hair production, and inhibition of primary roots and hemicellulose degradation (Ruotolo *et al*., 2018). Furthermore, Ruotolo *et al*. (2018) reported as several studies observed anomalous cells dimensions and structure, transcriptomic processes damages and problems to DNA packaging; other effects are represented by ribosome damaging with consequent energetic metabolism problems.

As reported by Ma *et al*. (2015), Zn oxides NPs can induce excess of ROS, cellular death, DNA damages, damages to pollen membranes and chlorophyll damages.

The study carried on by Gosh *et al*. (2016) highlighted how ZnO NPs tested on model plants *Allium cepa*, *Nicotiana tabacum* and *Vicia faba* can induce ROS formation and DNA damages such as chromosome aberration, micronucleus formation, and DNA stand-breaks. Another important biological response of tested model plants to ZnO NPs exposure is the increase of lipids peroxidation and the increase of antioxidant enzymes activity. Another evidence of Zn oxides ENM on plants was reported by Shaymurat *et al*., (2012); they reported as ZnO NPs induces several kinds of mitotic aberration (chromosome stickiness, bridges, breakage and laggings) on *Allium sativum*. Lee *et al*., (2013), using RAPDs, highlight differences in amplification profiles of *F. esculentum* roots cells exposed to 2000 mg/L of ZnO NP.

Similar increase of ROS concentration, lipids peroxidation and DNA insertion or deletion have been observed by Priester *et al*., (2017) in leaves of *G. max* exposed to nano-ZnO.

In both the cited studies, and in a review by Cox *et al*. (2016), the genotoxic effects of Zn NPs are likely due to the presence of ROS that produce oxidative stress of biomolecules.

As reported by Zuverza-Mena *et al*. (2017), effects of ZnO NPs are in general controversial. On *A. thaliana*, Zn based NMs caused genome alteration and downregulation of expression of genes involved in protein synthesis and biogenesis.

On *Pisum sativum*, lettuce, turnip and chicory it's been reported an inhibition of roots growth (500 ng/kg in soil), while in *Solanum licopersicum* it's been observed an increment of shoot growth and in leaf an increment of biomass, protein and chlorophyll concentration (250 ng/kg in soil) (Zuverza-Mena *et al*., 2017).

ZnO NMs can have even a negative effect also on plants rhizosphere damaging the interaction between microbes and plants and damaging N fixation.

1.4.4. CeO_2 Nanoparticles

Importantly, CeO_2 NPs are very stable in the environment, thus they can interact with several plants generation and release low quantities of Ce^{4+} ions, but in general, plants can uptake very high quantities of this NM (Zuverza-Mena *et al*.,

2017). Furthermore, it seems that the roots exudates increase the uptake of Ce based NPs (Zuverza-Mena *et al*., 2017) and always due to their persistence, they can be easily translocated from roots (Ma *et al*., 2018) or leaves (Ma *et al*., 2015) in the whole plant. However, the translocation on CeO_2 ENM is still controversial.

While Priester *et al*., (2017), after exposing plants of *G. max* to CeO_2 NPs, report that no mutagenic effects (DNA insertions or deletions) is observed, other studies, performed on the same model plant, highlight significant DNA damages.

Zuverza-Mena *et al*. (2017) reported how in *Oryza sativa*, watermelon and *S. lycopersicum* CeO_2 NM are highly accumulated in edible parts, while in *Z. mays* the accumulation occurs especially in the roots apparatus (Ma *et al*., 2015). Ma *et al*. (2018) reported as even in *L. sativa*, CeO_2 NPs are translocated from the roots to leaves after exposition concentration of 500 and 1000 mg/kg of soil.

Ma *et al*. (2015) reported also as, in *G. max* and *S. lycopersicum*, the XAS technique permitted to highlights a significant increase of CeO_2 NPs in fruits.

Furthermore, in *Phaseolus vulgaris* it's been reported an increase of seeds dimensions but a decrease of nutrient concentration (Zuverza-Mena *et al*., 2017).

Zuverza-Mena *et al*. (2017) reported also as Ce based NPs can induce ROS production with an increase of anti-oxidative defences.

Ruotolo *et al*. (2018) reported as, transcriptomic analysis performed on *A. thaliana* exposed to CeO_2 NPs, induces underexpression of genes involved in nutrients and water assumption, lateral roots and roots hair formation and xyloglucan metabolism. Contrarily, underexpression of genes involved in ROS detoxification, oxidative stress and systemic acquired resistance (SAR).

1.4.5. Ag Based Nanoparticles

Becaro *et al*., (2017) reported as Ag NPs, tested on the meristem cells of *A. cepa* roots, induces chromosome aberration and chromosome breakages. Similar results are reported by Sobieh *et al*. (2016) after testing Ag NPs on *A. cepa* roots cells and highlighting chromosome loss or chromosome breaking.

Another study by Çekiç *et al*. (2017) highlighted how the exposure to Ag nanoparticles of *S. lycopersicum* plants induces the formation of DNA mutation, likely due to an oxidative stress. Another confirm of Ag based NPs was provided by a study of Kumari *et al*., (2009), performed on *A. cepa*; in this study chromosome aberrations and breaks were observed among other effects on cell reproduction.

1.4.6. TiO_2 Nanoparticles

In their reviews, Cox *et al*. (2016) and Tripathi *et al*. (2017) reported as, in several studies performed on *A. cepa, Z. mais* and *Nicotiana tabacum*, Ti based NPs, especially in the form of TiO_2, can induce DNA damages as chromosome aberration. As other types of plants response to NPs exposure, the damage is likely indirect. In fact, the exposure to TiO2 NPs is often associate with ROS increase.

Silva *et al.* (2017) confirmed the genotoxicity of TiO_2, in a comparative study performed on *Lactuca sativa* and *Ocimum basilicum*, performing micronuclei test the presence of micronuclei in roots cells of *L. sativa* but not in *O. basilicum* when they were exposed to rutile + anatase TiO_2 NPs.

1.4.7. Iron based Nanoparticles

There are two principal types of Fe-based NM, Fe_3O_4 NM (nano-magnetite) and Fe_2O_3 NM, reported often as *n*FeO_x NM.

As reported by Zuverza-Mena *et al*. (2017), in general, *n*FeO_x NM are considered not very dangerous for plants because their scarce uptake and translocation. In fact, the majority of *n*FeO_x NPs are bigger than 20 nm so they can't easily cross cell walls and cell membranes.

As confirmed by Zuverza-Mena *et al*. (2017), the most important toxic effect of *n*FeO_x NM on plants is due to the aggregation of these materials on the roots surface with subsequent interference on water and nutrients uptake.

Specifically, for Fe_3O_4, it has been reported an increase of the concentration of antioxidant enzymes, an increase of lipid peroxidation, blocks of aquaporins and an increase of roots transpiration Zuverza-Mena *et al*. (2017).

Overall, these studies highlighted that the most frequent genotoxic effects are chromosomal aberrations, chromosomal breaking and micronuclei appearance that are, in general, investigated with the comet assay test or micronuclei test (Becaro *et al*., 2017; Gosh *et al*. 2016; Sobieh *et al*. 2016).

Another general feature of the phenomenon is that, genotoxicity, is principally due to the presence of ROS generated from the interaction between cells biomolecules and NM (de la Rosa *et al*., 2017; Hellack *et al*., 2017; Ma *et* al., 2015; Reddy *et al*., 2016; Tripathi *et al*., 2017).

Possibly, damages can be produce directly on DNA, if NM particles are sufficiently small (smaller than 8-10 nm) to cross nuclear membranes by diffusion or pore-crossing or altering physiological process such as replication of DNA or transcription of DNA into RNA (Martínez-Fernández *et al*. 2017).

1.4.8. Cadmium Sulphide Quantum Dots

CdS QDs represent one of the most interesting type of ENM, and one who there is an urgent need of investigation due to their increasing use in fields such drug delivery, medicine, semiconductor technology, photovoltaic cells and optical display applications (Pagano *et al*., 2018).

Recent studies (Marmiroli *et al*., 2014; Marmiroli *et al*., 2015) highlights several effects on *A. thaliana* w.t. exposed to 80 mg/L of CdS QDs for 21 d such decrease of photosynthetic activity, cellular respiration and biomass production in addition to modified expression of genes encoding for antioxidant enzymes and the production of anthocyanins (these last two effects are likely due to ROS activity). In these researches are highlighted also the interesting activities of chloroplast and mitochondrion in response to CdS QDs, and particularly the gene *ORF31*, which codes for an electron carrier located in the chloroplast endomembrane system and is part of cytochrome b_6f complex, was consistently modulated in response to ENM exposure (Pagano *et al*., 2018).

In order to reassume the genotoxic effects of several type of ENM on different species, Tab.1.1. was included.

Table 1.1. summary of the principal genotoxic effects highlighted by several studies on different plant species and for different ENM types.

ENM	*Plant Species*	*Effects*	*References*
CuO NPs	*Raphanus sativus* *Lolium perenne* *Lolium rigidum* *Fagopyrum esculentum* *Coriandrum sativum*	Chromosome breakage, micronuclei presence, difference in RAPDs profiles	Lee *et al*., (2013) Atha *et al*., (2012) Pramanik *et al*., (2017)
ZnO NPs	*Allium cepa* *Nicotiana tabacum* *Vicia faba*	Chromosome aberration, micronucleus formation, DNA stand-breaks	Gosh *et al*., (2016)
	Allium sativum	Chromosome stickiness, bridges, breakage and laggings	Shaymurat *et al*., (2012)
	Glycine max	DNA insertion or deletion	Priester *et al*., (2017)
CeO_2 NPs	*Glycine max*	DNA insertion or deletion	Priester *et al*., (2017)
Ag NPs	*Allium cepa*	Chromosome aberration and chromosome breakages	Becaro *et al*., (2017)
	Allium cepa	Chromosome loss or breaking	Sobieh *et al*. (2016)
	Allium cepa	Chromosomal aberration and breaks	Kumari *et al*., (2009)
	Solanum lycopersicum	DNA mutation	Çekiç *et al*. (2017)
Ti NPs	*Allium cepa*, *Zea mais*	DNA damages as chromosome aberration	Cox *et al*. (2016)
	Nicotiana tabacum		Tripathi *et al*. (2017)
	Lactuca sativa	Micronuclei presence	Silva *et al*. (2017)

1.4.9. Interactions Between Nanomaterials, Plants and Environment

As cited above, it could be very difficult to assess the behaviour of NM-plant-environment system because the features of the three components could interact in complex ways. Therefore, in this perspective only a holistic approach (principally given by long term studies) can provides useful results about the potential effects of

NM on soil health, soil microbial community and plants (Gardea-Torresdey *et al*., 2014).

In general, nanoecotoxicological studies performed on plants (that are the organisms at the food chains base) could provide good information about the potential trophic uptake and transfer in food chains (Martínez-Fernández *et al*. 2017, Ma *et al*., 2018).

Despite the increasing number of studies, a lot of controversial data are provided by researches because it seems that the response of plants to NM depends principally from many factors (Martínez-Fernández *et al*. 2017):

- physical and chemical properties of NM;
- concentration and dose of NM in the environment (high or low);
- time of exposure of the plants at NM;
- plant features (species, age, potential physiological status of stress);
- features of environmental matrix.

As reported by Gardea-Torresdey *et al*., (2014), plants could be exposed to NM in four different ways:

- through the direct application of agricultural lands;
- as nanoenabled agricultural products (pesticides, growth regulator or plant protectives);
- as soil remediation technologies;
- by atmospheric deposition, spillage, discharge, etc.

Some of the more important responses of the plant to an NM-contaminated environment could be a modification of the seed germination, alterations of nutrients and water uptake capacity, biomass and chlorophyll production, oxidative stresses and genotoxicity (Remédios, Rosário & Bastos, 2012; Martínez-Fernández *et al*., 2017; Wang *et al.,* 2013).

In first place, plants roots apparatus could interact with NM, at the level of the rhizosphere (the environment created from plants by production of exudates (phenols, aldehydes, organic acids) that confers bioavailability to both nutrients and toxic metals.

Then, there are three principal types of interaction between NMs and plant roots (Khan *et al*., 2017; Martínez-Fernández *et al*. 2017):

- adsorption on roots surface
- incorporation to the cell walls
- uptake into cells

However, the bioavailability of NMs for the uptake depends, as previously stated, from soil features and from the capacity of the plants to modify the rhizosphere conditions. In fact, as largely demonstrated for heavy metals, even for NMs some features changing (*e.g.* increase of bioavailability) could occur (Zhang *et al*., 2015).

If NM particles enter inside root apparatus, they could cause damages to cells (depending on their dimensions) by blocking pores, disrupting cell walls or aggregating at pores level causing problems in water balance and, consequently, at the nutritional state of plants.

In general, exposure to NMs involves changes in nutritional state, and development of plant is negatively affected, but positive effects are documented as well (Martínez-Fernández *et al*. 2017).

If NM particles are sufficiently small, they could be transported across the cortex by apoplastic/symplastic ways and reach the xylem cylinder.

Once arrived to the xylem system, NMs, could be transported in shoot or leaf apparatus by xylematic vessels transport (Khan *et al*., 2017; Zhang *et al*., 2015).

There might be also the possibility that a part of the transported NM could be translocated to seeds and transmitted to the progeny (Zhang *et al*., 2015).

Importantly, the capacity of plants to transport NMs, depends both to the plant species (plant anatomy and physiology) (Pacheco & Buzea, 2018), and NM type (dimension and reactivity) (Martínez-Fernández *et al*. 2017; Zhang *et al*., 2015).

ENMs inside plant cells can cause damages to photosynthesizing parts including the damage to the photosynthetic system (in general by interaction between NM and the proteins of photosystems) or in starch-synthetizing system (Martínez-Fernández *et al*. 2017).

In definitive, all the effects that NMs can provoke to plants results in a modification of the growth or development and in biomass production. In general, the modifications at plant growth depends strongly on the contest, in fact, as stated by Martínez-Fernández *et al*. (2017), is possible that a specific type of NM could cause damage to plants in some conditions but, in a different contest it's possible the it has a positive effect on growth.

1.4.10. Other Approach as Possible Support to ENMs Toxicity Assessment

Although not used in this work, it's important to notice that a possible alternative approach to assess ENMs toxicity is represented by QSAR, or quantitative structure activity relationship. QSAR is a statistical model that relates a set of structural or property descriptors of a chemical compound to its biological activity.

To establish the relationship between structure and activity, QSAR exploit information such as hydrophobicity, topology, electronic properties, steric effect (determined computationally or experimentally) and biological activity (determined with chemical analysis or biological essays). In general, QSAR models can be useful every time that toxicological tests are too much time-consuming and resource intensive (Burello, 2017). Nowadays QSAR are extensively used to predict toxic effects on environmental systems or organisms particularly where the toxicity endpoint is less understood (*e.g.* mutagenicity, carcinogenesis), and where no single interaction mechanism is previously known (Burello, 2017).

There are several problems in applying QSAR method to ENMs related to the fact that ENM share properties associated with both solutes and particles phases (Burello & Worth, 2011):

- Correct measures and characterization in environmental and biological matrices
- Correct preparation and testing for assessing bioavailability and effects

The level of knowledge of these crucial features might hinder the complete understanding of their mechanism of action, and the identification of descriptor able to describe their activity (Burello & Worth, 2011; Burello, 2017). Moreover, the quantity of information about ENMs are relative small if compared with information about conventional substances (Burello, 2017).

At the moment QSAR models applied to ENMs do not completely satisfied OECD parameters, and to improve the feasibility of this approach to OECD requests, a reliable set of data, collected from experiment performed in standardized conditions, is necessary. The usefulness of QSAR reach the best performances only if accompanied with standardized in vivo and in vitro experiments performed in laboratory but, in the future, they'll be likely able to predict properties of ENMs (Burello, 2017).

Data collected from this work and from other scientific articles can contribute to the development of reliable QSAR models on ENMs.

2. AIM OF THE STUDY

Since previous researches on the toxicity of metals cations Cd^{2+} from $CdSO_4$, compared with CdS QDs, highlighted the differences in responses on *Arabidopsis thaliana* (Marmiroli *et al*., 2014), the principal goal of this work is assessing the potential genotoxicity of a set of metal based ENM, compared with relative metals salts, in order to highlight differences between each compound, to contribute at the collection of data for future risk assessment procedure, and potentially providing indications for a more "safe by design" approach.

To reach this goal, two types of molecular markers were chosen to assess the genotoxicity of ENMs on genomic, chloroplastic and mitochondrial genome. To assess the potential effect on genomic DNA (mutations), random amplified polymorphic DNA primers profiles were analysed. At the same time, chloroplast and mitochondrial gene primers were used to assess the genotoxic effects (mutations and reorganizations) on the chloroplast and mitochondrial genome respectively. Considering these points, the study would like to highlight structural modification concerning genetic material.

The genotoxicity was chosen since, as previously outlined, this particular type of toxic effects related to ENMs is often related to oxidative stress and DNA mutations.

Moreover, as the principal topic of this work regards the environmental potential risk of ENM. The choice of the model plant *A. thaliana* was justified by the importance of this specie in genetic studies. Moreover, *A. thaliana* represent a model plant simulating the primary producer in the ecosystem through which ENMs can potentially enter in the food chain and arrive, trough bioaccumulation and biomagnification process, to higher trophic levels (Ahmed *et al*., 2018).

It's important to stress the concept of safe design of ENMs, since studying their effects on living organisms it's possible to highlight aspects important in several application fields, *e. g.* providing information for the use in agriculture of a more stable nanoform of a metal based chemical compound rather than salt form.

This work is structured in two different part:

1. The first part is focused on CdS QDs and $CdSO_4$ potential genotoxicity analysis on genomic, chloroplastic and mitochondrial genomes;
2. The second part consist in the extension of the genotoxicity analysis on a set of other metal based ENM (CeO_2 NM, Fe_2O_3 NM, Fe_3O_4 NM, ZnS QDs) and ($CeCl_3$, $FeCl_3$, $ZnSO_4$.

Finally, all collected data are simultaneously compared (and integrated with physiological data) using principal component analysis with the purpose of highlight potential similarity and differences on the base of plants genetic responses.

3. MATERIALS AND METHODS

3.1. TESTED ENMs CHARACTERIZATION

Particle agglomerates size, (*dh*), and ζ-potential are summarized in § 4.1, according to Pagano et al., 2017.

To measure the relative release of metal ions for tested ENM, flame atomic absorption spectrometry (FA-AAS) analyses were performed. These analyses permit to collect data relative to dissolution of ENMs in a medium (distilled water or Murashige and Skoog Basal Medium) and provide quantitative information about metal ions released in solution.

While CdS QDs and CeO_2 NMs were already analysed at FA-AAS (Pagano *et al*., 2017), ZnS QDs, Fe_2O_3 NMs, and Fe_3O_4 NMs weren't analysed n previous researches. Dissolution measures were performed starting from concentration of 500 mg/L (test concentration, see §4.2.), in both distilled water and MS, for each Zn and Fe based ENM at several times: 0, 1, 5, and 10 days after the suspension.The standards used for comparisons are Zn (Zinc) and Fe (Iron) standards (Agilent Technologies©, Santa Clara, CA, USA), prepared in conformity with instructions provided by the manual: Flame Atomic Absorption Spectrometry: Analytical Methods (2017). Agilent Technologies©, Inc. (Fe at p. 28, and Zn at p. 57). Zn standards are concentrated at 0,1; 0,5; 1 and 2 mg/L while Fe standards are concentrated at 0,1; 0,5 and 5 mg/L. Moreover, only MS solution was analysed as comparison for MS dissolution analyses. The protocol used for FA-AAS samples preparation is reported in Marmiroli *et al*., (2020).

PLANTS GROWTH CONDITIONS

Seeds of *Arabidopsis thaliana* (L.) Heynh. accession Landsberg erecta Ler-0 wild type were sown on Murashige and Skoog (MS) Basal Medium (SIGMA-ALDRICH™ Corporation, St. Louis, MO, USA) prepared with agar (0,8%) (SIGMA-ALDRICH™ Corporation, St. Louis, MO, USA), and D(+)-sucrose (1%) (PanReach AppliChem™, Chicago, IL, USA), at the density of 50 seeds for Petri dish (25 mL of MS for Petri dish).

Then, Petri dishes with seeds were maintained in growth chamber for 10 days (the first three days in complete darkness) at 16 h at 25°C in light, and 8 h at 19°C in dark.

Subsequently, in the first experiment performed, a part of plants was immediately harvested to obtain T0 samples, while the others plants were transferred on MS + CdS QDs at the concentrations of 0 (Cont.), 40, 80, 150 and 250 mg/L, and on MS + $CdSO_4$ (cadmium sulphate hydrate, SIGMA-ALDRICH™ Corporation, St. Louis, MO, USA) at the concentrations of 50 and 100 µM (density of 25 plants for Petri dish; 25 mL of growth medium for Petri dish).

Transferred plants were maintained in growth chamber for 10 days (T10 samples) and 20 days (T20 samples), at the conditions of 16 h in light at 25°C and 8 h in darkness at 19°C before harvesting.

In this way were obtained the following samples: T0, T10-Cont., T10-40, T10-80, T10-150, T10-250, T10-50Cd, T10-100Cd, T20-Cont., T20-40, T20-80, T20-150, T20-250, T20-50Cd and T20-100Cd. Each experiment was performed in triplicates.

For the second experiment performed on other ENM and salts, a similar procedure was followed but, since the number of compounds was extended, only 20 d were chosen to simulate a realistic chronic exposure time for *A. thaliana*. The ENMs tested in the second experiment are CeO_2 NM, Fe_2O_3 NM, Fe_3O_4 NM, and ZnS QDs. The salts are $FeCl_3$ (iron (III) chloride, SIGMA-ALDRICH™ Corporation, St. Louis, MO, USA), $ZnSO_4$ (zinc sulphate heptahydrate, SIGMA-ALDRICH™ Corporation, St. Louis, MO, USA), and $CeCl_3$ (SIGMA-ALDRICH™ Corporation, St. Louis, MO, USA). Concentration chosen in Ce, Fe and Zn based ENM were chosen on the base of repeated toxicity test in order to identify the Minimum Inhibition Concentrations (MIC) for each compound. Since the MIC of ENMs were often not realistic (higher then concentration generally detected in natural environments), 50% of the MIC were used in the experiments. In Tab. 4.4. are showed, for each compound, the tested concentrations.

3.2. DNA EXTRACTION PROCEDURE

To obtain the DNA, cetrimonium bromide or CTAB [$(C_{16}H_{33})N(CH_3)_3$] laboratory DNA extraction protocol was followed. The protocol steps are the following:

- Powdering of raw biological material with the use of ceramic pestles and mortars in presence of liquid nitrogen
- Addition of 0,9 mL of 2× CTAB extraction buffer (CTAB 2%, EDTA 20 mM, NaCl 0,7 M, Tris-HCl (pH 8) 100mM) at 0,2 g of powdered sample
- Addition of 4,5 µL of Proteinase K from *Tritirachium album* (SIGMA-ALDRICH™ Corporation, St. Louis, MI, USA), and incubation for 30 min at 65°C
- Addition of 3 µL of RNase A Solution (Promega™, Madison, WI, USA), and incubation for 30 min at 65°C
- Recovering of supernatant and addiction of 800 µL of chloroform: isoamyl acid (24:1)
- Centrifugation at 15°C, and 13000 rpm, for 5 min (step performed 2 times)
- Addition of 1 mL of cool isopropanol
- Precipitation for 2 h at -20°C
- Centrifugation at 4°C, and 13000 rpm, for 20 min (step performed 2 times)
- Removal of supernatant and drying of pellet at 37°C for 1 h
- Resuspension of pellet in 50 µL of distilled water

3.3. PCR BASED METHODS

The principle on which PCR-based methods are based, consist in the catalysis performed by DNA polymerase that allows the elongation of DNA molecules.

In the presence of a primer and a DNA template, DNA polymerase catalyses the synthesis of a complementary DNA sequence. Repeated cycles of denaturation, annealing, and extension result in the exponential amplification of one or several specific (in the case of RAPD, not specific) DNA.

The resulting amplified bands are specific to the original DNA template and can be used as genetic markers (Cloutier & Landry, 1994).

3.4. RAPD PRIMERS SELECTION

For analysis of potential genotoxic effects of ENM and salts on nuclear genome, the PCR based technique of Random Amplified Polymorphic DNA (RAPD) analysis was performed. The use of RAPD was justified by the fact that they allow to explore a wide genome (they're not specific of any DNA regions) in relative brief time, that make RAPD particularly feasible for a preliminary genome wide study.

Essentially RAPD markers represent a variation of the PCR, where a single primer of an arbitrary nucleotide sequence is used to drive the amplification reaction. An important feature of RAPD technique is that, DNA fragments generated by amplification with arbitrary primers, often contain repetitive DNA sequences. In general, numerous RAPD markers can be quickly produce since no target DNA sequence information is needed (Cloutier & Landry, 1994). Furthermore, RAPD are dominant molecular marker; in fact, with their use, it's impossible to distinguish between heterozygotes and homozygotes genotypes.

So, for their features, RAPD analysis is a relatively simple, rapid and low-cost technique that do not require any type of previous knowledge about the organism genome. Furthermore, this technique allows to highlight a wide range of DNA damage (*e.g.* point mutations, inversion or deletions) and, at the same time a large number of samples can be investigated (Aras *et al*. 2012).

Recently, in a study performed on *V. faba* exposed to chlorinate wastewater, Mattar *et al*., (2015), demonstrated the effectiveness of RAPDs method to investigate on polymorphism induced by pollutants confirming *V. faba* as good bioindicator.

Importantly, despite their extended use, this technique has attracted some criticism, especially due to their effective reproducibility but recent studies have highlighted how, after a proper and appropriate optimization, RAPD represent a reliable, sensitive and reproducible assay (Atienzar & Jha, 2006), as demonstrated in studies performed on several higher plants species (Conte *et al*., 1998, Aras *et al*. 2012) to investigate the potential genotoxic effects of metals. Successful results performed on detection of mutations induced by ENM, in buckwheat, has been reported also by Lee *eta al*. (2013).

An initial set of 34 primers (14 of them chosen from Conte *et al*., 1998, while the others 20 was provided by SIGMA-ALDRICH™ Corporation, St. Louis, MO, USA) was tested, and finally 15 of them was selected for the reliability of produced profiles obtained. The sequence of each primer is shown in Tab. 3.3.

Table 3.1. In this table are listed, for each of most reliable 15 primer, the name and the 5' – 3' sequence.

Primer Name	**Sequence (5' – 3')**
OPA-05	AGGGGTCTTG
OPA-07	GAAACGGGTG
OPA-08	GTGACGTAGG
OPA-10	GTGATCGCAG
OPB-01	GTTTCGCTCC
OPB-07	GGTGACGCAG
OPG-02 (Conte *et al*. 1998)	GGCACTGAGG
OPG-06	GTGCCTAACC
OPG-10	AGGGCCGTCT
OPG-16	AGCGTCCTCC
OPG-19	GTCAGGGCAA
OPAS-09	TGGAGTCCCC
OPAS-12	TGACCAGGCA
OPAS-14	TCGCAGCGTT
OPAS-15	CTGCAATGGG

3.5. END POINT PCR PROTOCOL

RAPDs analyses were performed at end-point PCR, at the primer concentration of 250 nM. Amplification process was guaranteed by Colorless GoTaq Master Mix 2× (Promega™, Madison, WI, USA). The analyses were performed on Veriti™ 96-Well Thermal Cycler (Thermo Fisher Scientific™, Waltham, MA, USA).

The end point PCR steps performed are the following:

- Initial Denaturation: 1 cycle at 95°C for 2 min
- Amplification: 40 cycles (30 s at 95°C, 30 s at 35°C, 4 min at 72°C)
- Final Extension: 1 cycle at 72°C for 5 min
- Final Hold: 1 cycle at 4°C

After PCR, amplicons were subjected to electrophoresis run in agarose gel (agar 2%, 10 μL of GelRed™ Nucleic Acid Gel Stains (Biotium™, Fremont, CA, USA)).

3.6. REAL TIME QUANTITATIVE PCR

The real time quantitative PCR method is based on the fact that there is a quantitative relationship between the amount of starting target sequence and amount of PCR product (monitored with the use of a fluorescent detector) accumulated at any particular cycle.

The threshold cycle (Ct) is the central parameter that must be monitored during a real-time quantitative PCR, since it represents the fractional PCR cycle number at which, the reporter fluorescence, is greater than the minimal detection level (called threshold).

The presence of more template at the start of the reaction leads to a fewer number of cycles reaching the point the fluorescent signal is recorded as statistically significant above the background.

As the reaction components became limiting, the rate of target amplification decreases until the PCR reaction is no longer generating template at an exponential rate (final plateau phase of the fluorescent signal) and there is little or no increase of PCR product. During the exponential phase, that precedes the plateau phase (Fig.

3.4.), none of the reaction components is limiting and therefore Ct values are very reproducible for replicate reactions with the same starting copies number (Arya *et al*., 2005).

Figure 3.4. In this figure is outlined a model of single amplification plot obtainable with real-time quantitative PCR and reported the nomenclature of every phase of the process. ΔRn is the fluorescent emission of the product at each time point-fluorescence calculated from the software starting from the Rn, or the difference between Rfn (the fluorescent emission of the product at each time point) and Rnb (the fluorescent emission of the baseline) (www.ncbi.nlm.nih.gov).

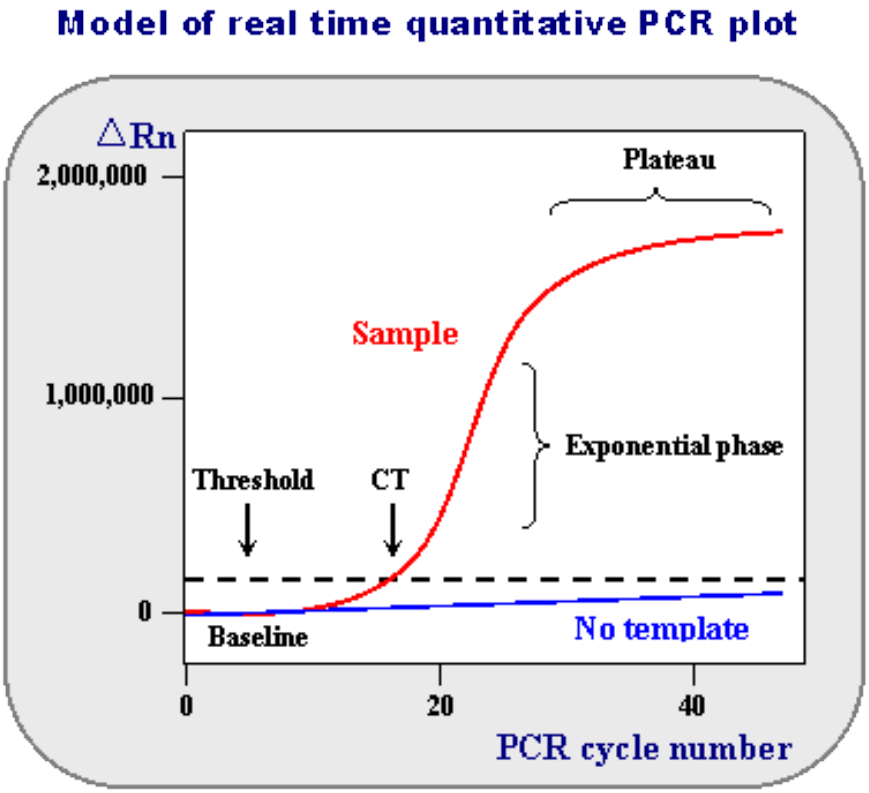

3.7. GENOMIC, MITOCHONDRIAL, AND CHLOROPLASTIC GENES PRIMERS SELECTION

For the analysis of the potential genotoxicity of ENM and salts on mitochondrial and chloroplast genetic material, a set of 11 primers (SIGMA-ALDRICH™ Corporation, St. Louis, MO, USA) was selected.

In order to cover in a homogeneously way both genomes, the investigated genes were selected on the only structural base; so, the choice of each gene has been done on the base of the position (Fig. 3.2.).

The complete gene names, and genetic ontologies of each gene are summed up in Tab. 3.5.

Table 3.2. In this table are listed, for each mitochondrial (mt), and chloroplast (chl) genes chosen for the real time quantitative PCR, the respective complete gene names and gene ontologies (all data from www.arabidopsis.org except for *ORF31* data from string-db.org).

Gene Id	Gene Name	Gene Ontology
COB (mt)	*Apocytochrome B*	Aerobic respiration, mitochondrial electron transport, encoding a subunit of the ubiquinol-cytochrome c oxidoreductase
COX (mt)	*Cytochrome Oxidase*	Encoding the cytochrome c oxidase subunit 1, aerobic respiration, mitochondrial electron transport, oxidative phosphorylation
CCB206 (mt)	*Cytochrome C Biogenesis 206*	Encoding a mitochondria-encoded cytochrome c biogenesis 206, heme transport, and transmembrane transport
CCB256 (mt)	*Cytochrome C Biogenesis 256*	Cytochrome complex assembly, heme transport
CCB382 (mt)	*Cytochrome C Biogenesis 382*	Cytochrome complex assembly, heme transport
YCF1 (chl)	*YCF1.1*	Encoding the Ycf1 protein, involved in guard cells function
PSBA (chl)	*Photosystem II Reaction Center Protein A*	Encoding the chlorophyll binding protein D1, a part of the photosystem II reaction center core, involved in photosynthetic electron transport in photosystem II, and response to herbicides
PSBD (chl)	*Photosystem II Reaction Center Protein D*	Involved in photosynthetic electron transport in photosystem II
PSBF (chl)	*Photosystem II Reaction Center Protein F*	Photosynthetic electron transport chain
ORF31 (chl)	*AtCg00590*	Encoding the cytochrome b6f-complex subunit 6 (*PetL*) which mediates electron transfer between photosystem II (PSII) and photosystem I (PSI)
PSAC (chl)	*PSAC*	Encoding the PsaC subunit of photosystem I, photosynthetic electron transport in photosystem I

The nucleotide sequence of genes was analysed on the website www.arabidopsis.org, while the most suitable primer length (considering the

temperatures of PCR process, and the reduction of spurious annealing) was obtained with the use of the website primer3.ut.ee. The primers sequences are listed in Tab. 3.6.

Table 3.6. In this table are listed, for each of the organellar (Org), mitochondrial (Mt) and chloroplast (Cp) genes chosen for the real time quantitative PCR, forward and reverse primers sequence.

Gene Name	Forward sequence (5' - 3')	Reverse Sequence (3' - 5')
COB (Mt)	CTAATCCGATGTCCACCCCG	TACACCTCCCGCTTTGTCAG
COX (Mt)	AACATGCGTGGACCTGGAAT	GCCAGTACCGGGAGTGATAAT
CCB206 (Mt)	GGAGCCTGGTCTTGACTCTT	TGGTTGGATTTTGCGAGCTG
CCB256 (Mt)	TCCCCTTTATCTTCGCTCTTCC	ATTGGTCTTCCCCGAAACCC
CCB382 (Mt)	TCAAACATGTGGGCGCAAAA	CCAGAACGAAGAGAAGGCGA
YCF1 (Cp)	GTCGTTGTGGTCGGACTCTA	CGGTTCCTTCTTCTCCTTCGT
PSBA (Cp)	TCCAGGCTGAGCACAACATT	GTTACCAAGGAACCATGCATAGC
PSBD (Cp)	GCGCCTAGTTTTGGTGTAGC	CGGCGACTCCCATCATATGA
PSBF (Cp)	CGCTGGTTGGCTGTTCATG	ACTGCATTGCTGATATTGACCC
ORF31 (Cp)	TAACTAGTTATTTCGGTTTTCTACTAGC	AGTCGTATTTTGCTTAGACCAATAAAC
PSAC (Cp)	CTCAATGTGTCCGAGCATGC	ACCAACACAGTCCTCGGTTC

The choice of the organellar gene *16S* as reference gene is justified by its stability, and relative smaller variability in Ct, in control and treatments assessed trough repeated real time PCA experiments. Starting from the position of *ORF31* on the *A. thaliana* chloroplastic DNA, the other five Cp genes were chosen to cover homogeneously the entire chloroplastic genome (Fig. 3.5.). The choice of *ORF31* was dictated by the fact that, several previous studies, demonstrate the involvement of this gene in metal based ENM responses (Marmiroli *et al*., 2014; Wang *et al*., 2016), while other researches highlight how is preserved in different plant species (Pagano *et al*., 2016; Pagano *et al*., 2017)

The choice of the five Mt genes was performed following the same concept (Fig. 3.6.).

Figure 3.5. Chloroplastic genome of *A. thaliana*, red arrows highlight the position of Cp genes chosen to assess the potential ENM genotoxicity on chloroplast genetic material (Cincu, 2014).

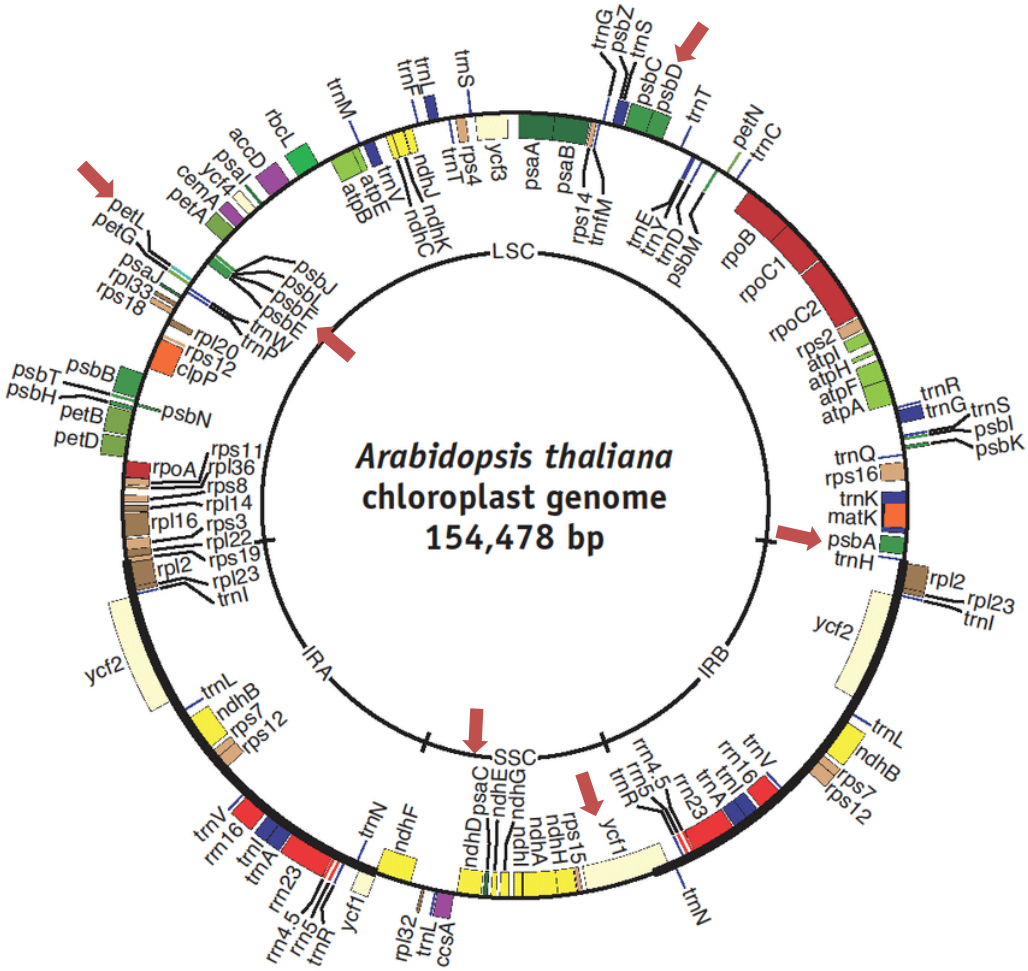

Figure 3.5. Mitochondrial genome of *A. thaliana*, red arrows highlight the position of Mt genes chosen to assess the potential ENM genotoxicity on mitochondrion genetic material (Cincu, 2014).

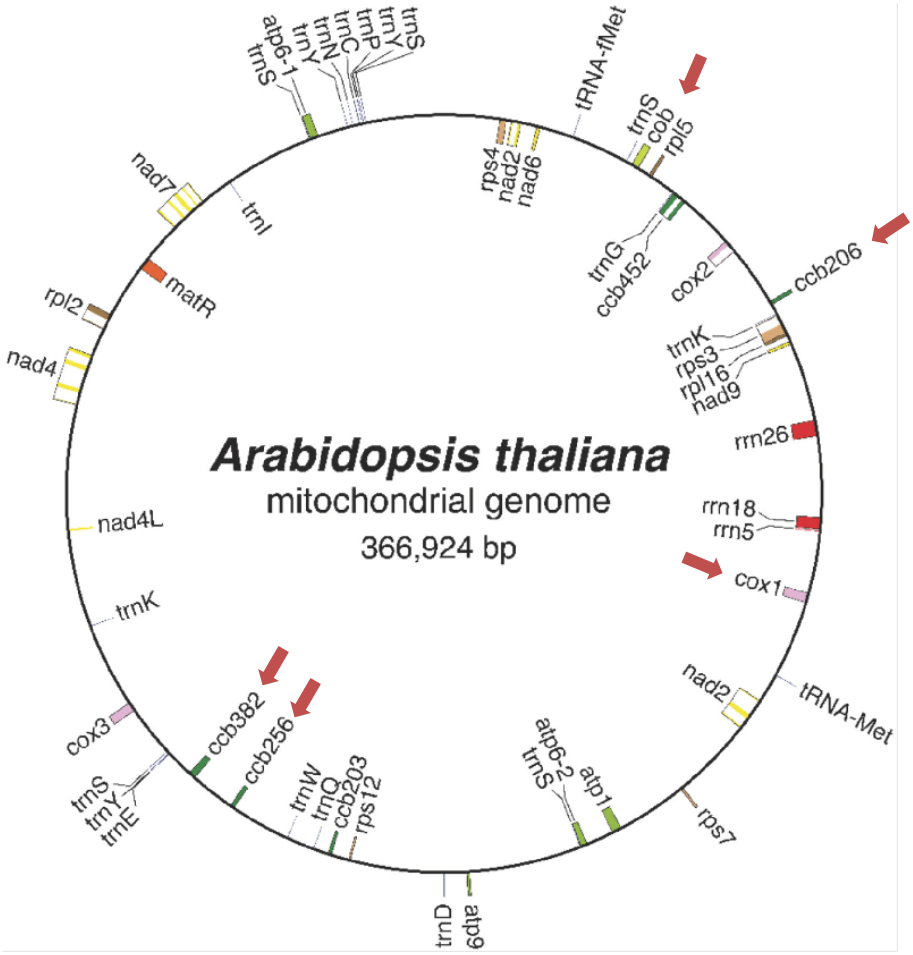

3.8. REAL TIME QUANTITATIVE PCR PROTOCOL

Mitochondrial and chloroplast analyses were performed at real-time quantitative PCR, at the concentration of 125 µM (in tripled), for both reverse and forward primers (in 10 µL of total volume).

Fluorescent signal detection was allowed by Power SYBR™ Green PCR Master Mix 2× (Applied Biosystem™, Foster City, CA, USA). The real time quantitative PCR was monitored with ABI Prism™ 7000 Sequencer Detection System using 7000 System SDS Software™ (Thermo Fisher scientific™, Waltham, MA, USA).

The real-time quantitative PCR steps performed are the following:

- Initial Denaturation: 1 cycle at 95°C for 3 min

- Amplification: 40 cycles (15 s at 95°C, 1 min at 60°C)
- Final Hold: 1 cycle at 4°C

3.10. MONODIMENSIONAL, MULTIDIMENSIONAL STATISTICAL ANALYSIS AND HEATMAPS GRAPHICAL REPRESENTATION

The RQ of every gene analysed in real time q-PCR was calculated starting from the respectively Ct media of tripled. Using the formula:

$$RQ = 2^{-\Delta\Delta Ct} \quad (3.1)$$

Were ΔCt is the differences between a specific gene and the reference gene for the same treatment, and ΔΔCt is the difference between the ΔCt of a specific treatment and the control for the same gene.

After the calculus, each RQ was normalized subtracting 1 from the calculated value. This transformation permit, in a clearer way, to establish what genes are overabundant and what underabundant referring to reference gene, but the significance of the differences must be verified with the use of an adequate statistical test.

To assess the statistical significance in differences, between the RQ of reference genes and mitochondrial or chloroplast genes, a *t* Student test was performed on raw data. Hereafter, the symbols *, **, and *** will be used to indicate the *t* Student test probabilities (p) < 0,05, < 0,01, and < 0,001 respectively.

The choice of *t* Student test is justified by the fact that a great variability in growth condition, and exposure time of plant responses was attended; consequently, statistical test was performed between the reference gene Ct, and each mitochondrial and chloroplast gene Ct. Every *t* Student test was performed using the software Microsoft® Office Excel (Microsoft®, Redmond, WA, USA).

To highlight latent variables able to describe the greater portion of data variability, a principal component analysis (PCA) was performed. PCA is a multidimensional statistic test permitting to describe the observed data variability

through a relative small number of fictitious dimensions (principal components), created from a linear combination of initial real dimensions that characterize every observation in a multidimensional space (in this case the real dimensions are ENM concentrations, exposure times, ENM types). PCA allows to describe how data are preferentially disposed with a relative smaller number of new variables starting from initial set of variables, and quantifying how initial variables, measured for every observation, ere related one each other. PCA analyses are performed with the use of statistical software R® version 3.5.1 (Feather Spray).

To highlight graphically the differences in relative number of copies between studied genes an heatmap representation was used. The intensity of colours in heatmaps is proportional to differences in relative number of copies (shades of green for the decrease, and shades of red for increase in respect to the reference gene). Heatmaps were designed with the use of statistical software R® version 3.5.1 (Feather Spray).

3.11. MORPHOLOGICAL AND PHYSIOLOGICAL ANALYSES

To support genetic analyses, in the second experiment performed, a panel of morphological and physiological parameters were measured. The morphological parameter is represented by biomass quantity, while physiological parameters includes chlorophyll a, chlorophyll b, and carotenoids concentrations, respiration rate (2,3,5-triphenyl-2H-tatrazolium chloride, or TTC, protocol) and lipid peroxidation (malondialdehyde, or MDA, protocol).

All the analyses were performed with the use of Varian ™ UV Spectrophotometer and Varian Cary WinUV Software (Varian Medical Systems™, Palo Alto, CA, USA).

3.12. PHOTOSYNTHETIC PIGMENTS PROTOCOL

The steps of photosynthetic pigments protocol (adapted from Marmiroli *et al*., 2020) are the following:

- Powdering of raw biological material with the use of ceramic pestles and mortars in presence of liquid nitrogen
- Addition of 1,8 mL of acetone

- Agitation, and cooling for 10 min in ice
- Centrifugation at 13000 rpm for 10 min
- Separation of extract photosynthetic pigments from solid residues
- Spectrophotometer measuring of chlorophyll a (662 nm), chlorophyll b (647) and carotenoids (480).

3.13. TTC PROTOCOL

To measure the rate of respiration, a TTC protocol was followed (Marmiroli *et al*., 2014; Marmiroli *et al*., 2020). The reduction reaction of the TTC to 1,3,5-triphenyltetrazolium formazan is an irreversible biochemical process that makes this chemical compound a reliable redox indicator of cellular respiration rate (Fig. 3.5.).

Figure 3.5. In this figure is schematically represented the reduction reaction of TTC that produce 1,3,5-triphenyltetrazolium formazan (cdn.biologydiscussion.com).

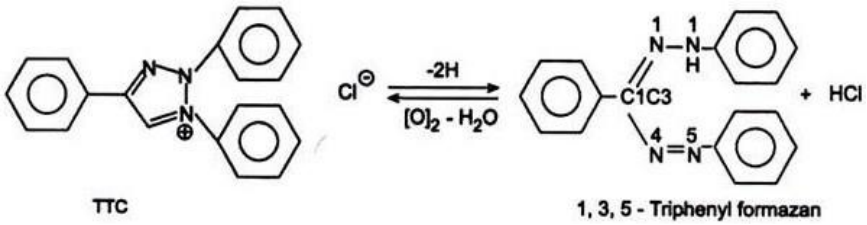

The TTC protocol steps are the following:

- Addition of TTC (0,18 M) at the solution buffer (78% $Na_2HPO_4 \cdot 2H_2O$ 0,05 M, 22% KH_2PO_4 0,05 M)
- Homogenization of 150 mg of biological material in 3 mL of TTC
- Incubation for 15 h at 30°C
- Recovering of biological material and washing with distilled water
- Addition of 7 mL of ethanol (95%) and incubation in bath for 5 min at 80°C
- Sample cooling in ice, and adding 3 mL of ethanol (95%) to reach 10 mL of ethanol
- Spectrophotometer measuring at 530 nm of wave length

3.14. MDA PROTOCOL

To measure the lipids peroxidation an MDA (chemical formula $CH_2(CHO)_2$) protocol was followed (Marmiroli *et al*., 2017; Marmiroli *et al*., 2020). MDA, reacting with thiobarbituric acid (TBA), forms MDA-TBA2 (Fig. 3.6.) that represent a reliable product of lipid peroxidation of polyunsaturated fatty acids. Furthermore, it represents a good marker to investigate the oxidative stress.

Figure 3.6. In this figure is schematically represented the MDA/TBA reaction that produce the MDA-TBA2 (www.nwlifescience.com).

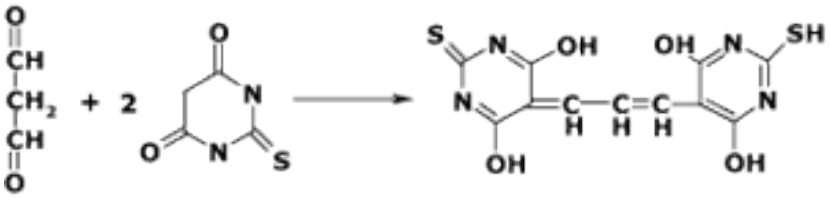

The MDA protocol steps are the following:

- Homogenization of 0,2 g of powdered sample with 1 mL of TCA solution (0,1% w/v)
- Centrifugation at 12000 rpm for 15 min
- Taking of 500 µL of supernatant, and addition of 1 mL of TBA solution (0,5% w/v) in TCA solution (20% w/v)
- Incubation at 95°C for 30 min
- Reaction blocking and cooling of samples in ice
- Centrifugation at 3000 rpm for 10 min
- Spectrophotometer measuring at 532 nm of wave length

4. RESULTS AND DISCUSSION

4.1. ζ-POTENTIAL AND DISSOLUTION ANALYSIS RESULTS

ENMs data relative to ζ-potential, *dh* are reported in Tab. 4.1.

Table. 4.1. In this table values of most important physical parameters for each tested ENMs are summarized.

ENMs	Size (nm)	(ζ) Z-potential (mV)*	(*dh*) hydrodinamic range (nm)*	% Metal
CdS QDs	<5	+ 15.8	178.7	78
ZnS QDs	<5	+ 61.6	1190	63.2
Fe_2O_3 NPs	<15	+ 3.8	978	69.8
Fe_3O_4 NPs	<10	+ 44.2	271.6	72.4
CeO_2 NPs	<25	+ 42.5	243.9	81.3

*ζ and *dh* measured in ddH_2O, pH = 7

Zn data collected from FA-AAS analyses are showed in Tab. 4.1., and Fe data are showed in Tab. 4.2. As it is possible to see, there are no relevant differences between media and times relative to ZnS QDs solutions, in fact concentrations detected with FA-AAS are similar each other. These results suggest how Zn^{2+} ions released by ZnS QDs it's not variable with time and substantially independent from the type of media used in the experiments.

Table 4.1. For each treatment of ZnS QDs, in both distilled water and MS, for different time lapses (0, 1, 5 and 10 days), are reported the percentages of dissolution respect the initial concentration of 500 mg/L. Standards and only MS data are reported.

Zn QDs		
Sample Name	**% of Dissolution**	**FA-AAS Analyses**
Standard 1	0,1	0,01
Standard 2	0,5	0,21
Standard 3	1	0,45
Standard 4	2	0,83
ZnS QDs + H_2O T0	0	0
ZnS QDs + H_2O T1	0,002	0,0097
ZnS QDs + H_2O T5	0,01	0,0262
ZnS QDs + H_2O T10	0,01	0,0354
ZnS QDs + MS T0	0	0
ZnS QDs + MS T1	0,01	0,0273
ZnS QDs + MS T5	0,01	0,0465
ZnS QDs + MS T10	0,01	0,026
MS	0	0

In Tab. 4.2. it is possible to observe how, similarly at Zn based ENM, differences between media and times, for both Fe_2O_3 and Fe_3O_4 NM, are not relevant.

Even in this case, Fe^{2+} and Fe^{3+} ions released by Fe based ENM seem not to depend from time and media chemical composition.

Table 4.2. For each treatment of Fe_2O_3 and Fe_3O_4 NM, in both distilled water and MS, for different time lapses (0, 1, 5 and 10 days), are reported the percentages of dissolution respect the initial concentration of 500 mg/L. Standards and only MS data are reported.

Fe_2O_3 NM – Fe_3O_4 NM		
Sample Name	**% of Dissolution**	**FA-AAS Analyses**
Standard 1	0,1	0,0004
Standard 2	0,5	0,0274
Standard 3	5	0,3648
Fe_2O_3 NM + H_2O T0	0,01	0,0632
Fe_2O_3 NM + H_2O T1	0,02	0,0741
Fe_2O_3 NM + H_2O T5	0,01	0,0206
Fe_2O_3 NM + H_2O T10	0,001	0,0057
Fe_2O_3 NM + MS T0	0,01	0,0417
Fe_2O_3 NM + MS T1	0,01	0,0396
Fe_2O_3 NM + MS T5	0,01	0,0284
Fe_2O_3 NM + MS T10	0,01	0,0358
Fe_3O_4 NM + H_2O T0	0,01	0,0375
Fe_3O_4 NM + H_2O T1	0,01	0,0289
Fe_3O_4 NM + H_2O T5	0,002	0,0135
Fe_3O_4 NM + H_2O T10	0,01	0,0295
Fe_3O_4 NM + MS T0	0,004	0,0181
Fe_3O_4 NM + MS T0	0,01	0,0431
Fe_3O_4 NM + MS T0	0,01	0,0324
Fe_3O_4 NM + MS T0	0,01	0,0352
MS	0,0004	0,0022

FA-AAS analysis allowed to highlight how the concentrations of dissolved metal ions, compared with the concentrations of ENM, are relatively small even considering the relative instability of Fe and Zn based ENM.

In conclusion, it is possible to state that the release of metal ions by Zn and Fe ENM is relative restrained.

4.2. CdS QDS RESULTS

As aforementioned in Chapter 2., the first experiment performed concerns the analyses of the DNA extracted from plants exposed to CdS QDs and $CdSO_4$ salt.

Tested concentrations were chosen on the base of previous results in literature (Marmiroli *et al*., 2014), where minimum inhibitory concentration (MIC) for CdS QDs (80 mg/L) and $CdSO_4$ (200 mg/L) were identified. As previously specified, concentrations of 0 (Cont.), 40, 80, 150 and 250 mg/L were tested for CdS QDs, while concentrations of 50 and 100 µM were tested for the corresponding salt $CdSO_4$.

4.2.1. RAPDs Results

Analysis were performed on each of the RAPDs listed in Tab. 2.1., for tested concentrations. After End Point PCR and electrophoresis run on agarose gel. Profiles of each sample were compared with the control profile.

In these comparisons the number, presence or absence of bands in amplicons, were checked to understand if the treatment influenced the annealing of primers to DNA highlighting potential mutations.

I Fig. 4.1. Is possible to see how, *OPA10*, allows to highlights a heavier band in both duplicated samples of T20-$CdSO_4$ 100 treatment, that doesn't compare in others samples (highlight in red). Contrariwise, T20-$CdSO_4$ 100 doesn't show the bands present in all other profiles.

Other profiles seem not to show prominent differences from each other and in comparison with the control. Differences in bands intensity could be due to differences in DNA concentrations principally influenced by treatments.

Figure 4.1. In this image is reported results obtained for RAPD *OPA10*. 50 bp ladder was used as reference, b. is the blanc sample.

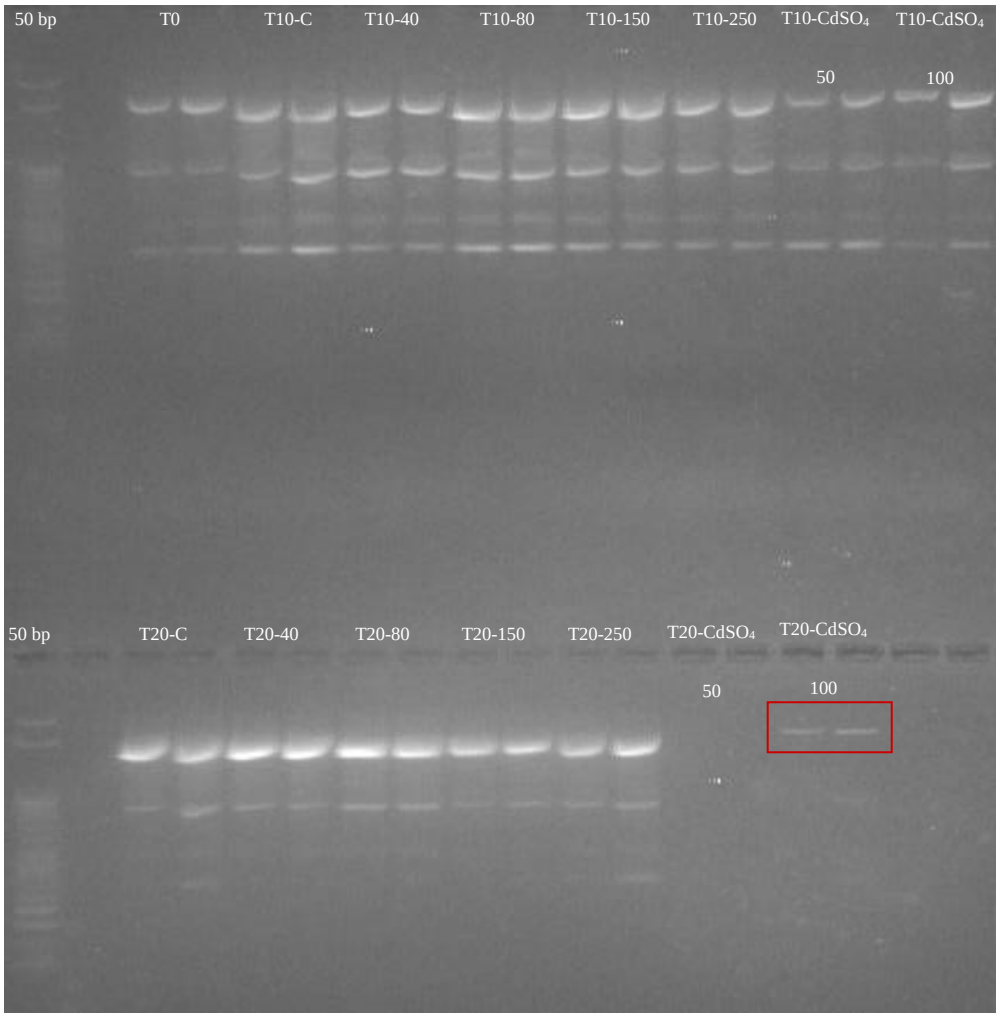

Other RAPDs markers that provide profiles with a relative higher number of bands, if compared with other primers, were *OPG2* (seven bands) and *OPG16* (ten bands).

Contrary to *OPA10*, *OPG2* and *OPG16* did not permit to highlight differences between control and treated (respectively Fig. 4.2. and Fig. 4.3.). Even in these cases the differences in bands brightness could be due to differences in DNA concentrations influenced by treatments.

Figure 4.2. In this image is reported results obtained for RAPD *OPG2* performed on a part of treated plants DNAs. 1 kb ladder was used as reference, b. is blanc sample.

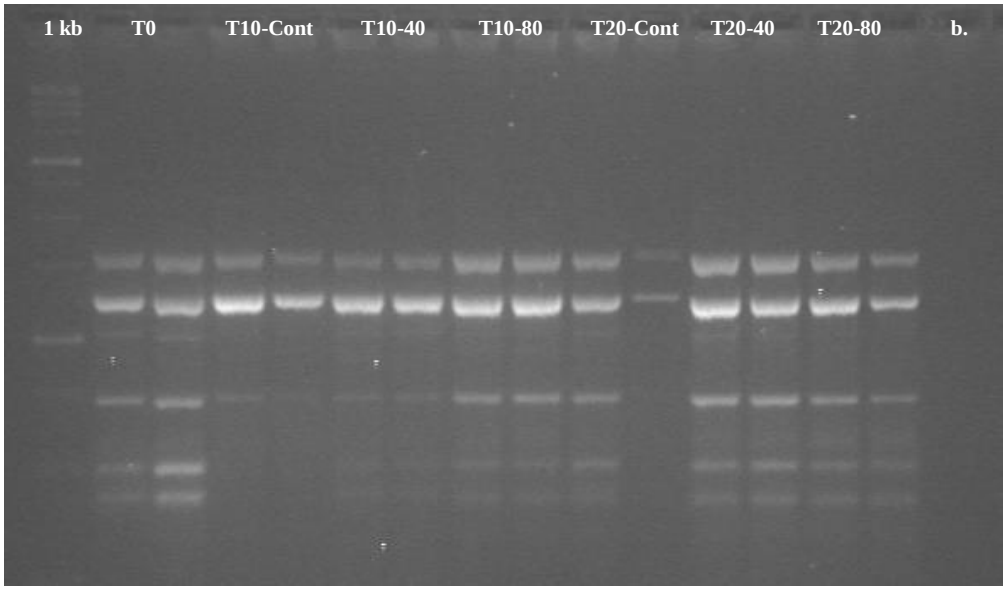

Figure 4.3. In this image is reported results obtained for RAPD *OPG16* performed on a part of treated plants DNAs. 1 kb ladder was used as reference, b. is the blanc sample.

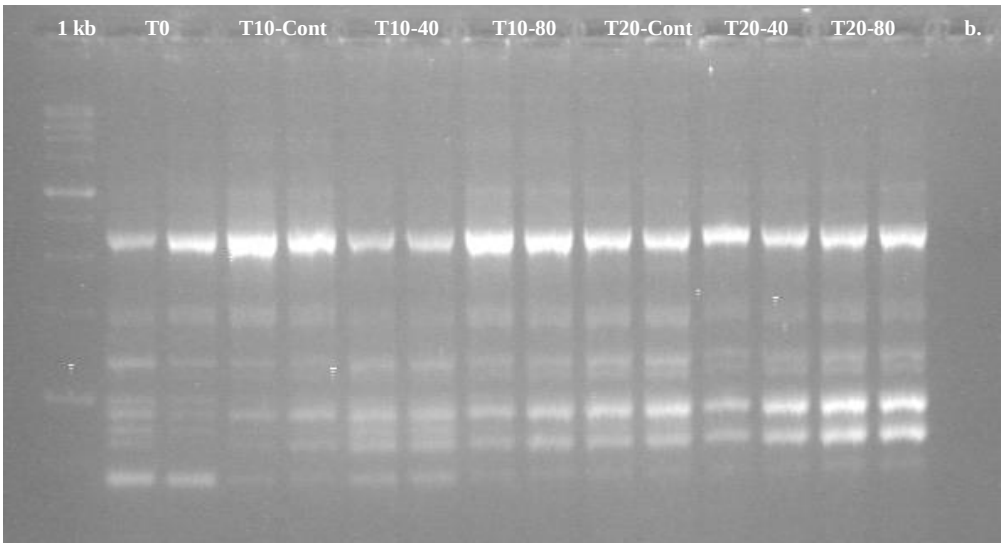

Based on these results, it is possible to understand how RAPDs analyses permit to investigate the whole genome of plants. Nevertheless, not all RAPDs permit to highlight differences between treatments profiles.

However, from these data it is possible to state that $CdSO_4$ treatments, for which the release of Cd^{2+} ions is relative high, the possibility to find mutations is higher if compared with CdS QDs that show a major stability with consequent lower release of toxic ions.

4.2.2. Real Time qPCR Results on Chloroplast and Mitochondrial Genes

Real Time qPCR analyses were performed on 11 genes (5 mitochondrial genes, and 6 chloroplastic genes) to highlight difference between relative number of copies in comparison with the reference gene *16S* (organellar). These analyses were performed starting from DNA extracted with CTAB protocol, as explained in §3.3.

Below, are showed results concerning the experiments on chloroplastic and mitochondrial genes respectively.

In Fig. 4.4. the heatmap shows the relative number of copies, of chloroplastic genes, for each treatment, while in Tab. 4.3. relative significance values are listed. CdS QDs treatments at higher concentrations induce a significant decrease in relative number of copies especially in *PSAC* (T10-250, T20-150, and T20-250). Then, gene *PSAC* seems to be more sensible to higher concentrations of CdS QDs. Similarly, gene *YCF1* gives significant results to higher concentrations of CdS QDs in both 10 and 20 days of exposure. In this way both *YCF1* and *PSAC* seem to be more sensible to acute toxicity induced by CdS QDs.

Conversely, *PSBA* shows significant increase in relative number of copies in CdS QDs treatments, principally at longer exposure times (T20-40, T10-80 and T20-80). These facts induce to consider *PSBA* more sensible to higher exposure times.

The gene *PSBD* seems to have a similar trend as *PSBA*, in fact it seems to be significantly more abundant in treatments with higher exposure times, and consequently, their sensibility to chronic toxicity induced by CdS QDs.

Figure 4.4. Heatmap of chloroplastic genes relative number of copies (normalized on T10-C), for each Cd based treatment. Data are presented as Log_{10}(RQ).

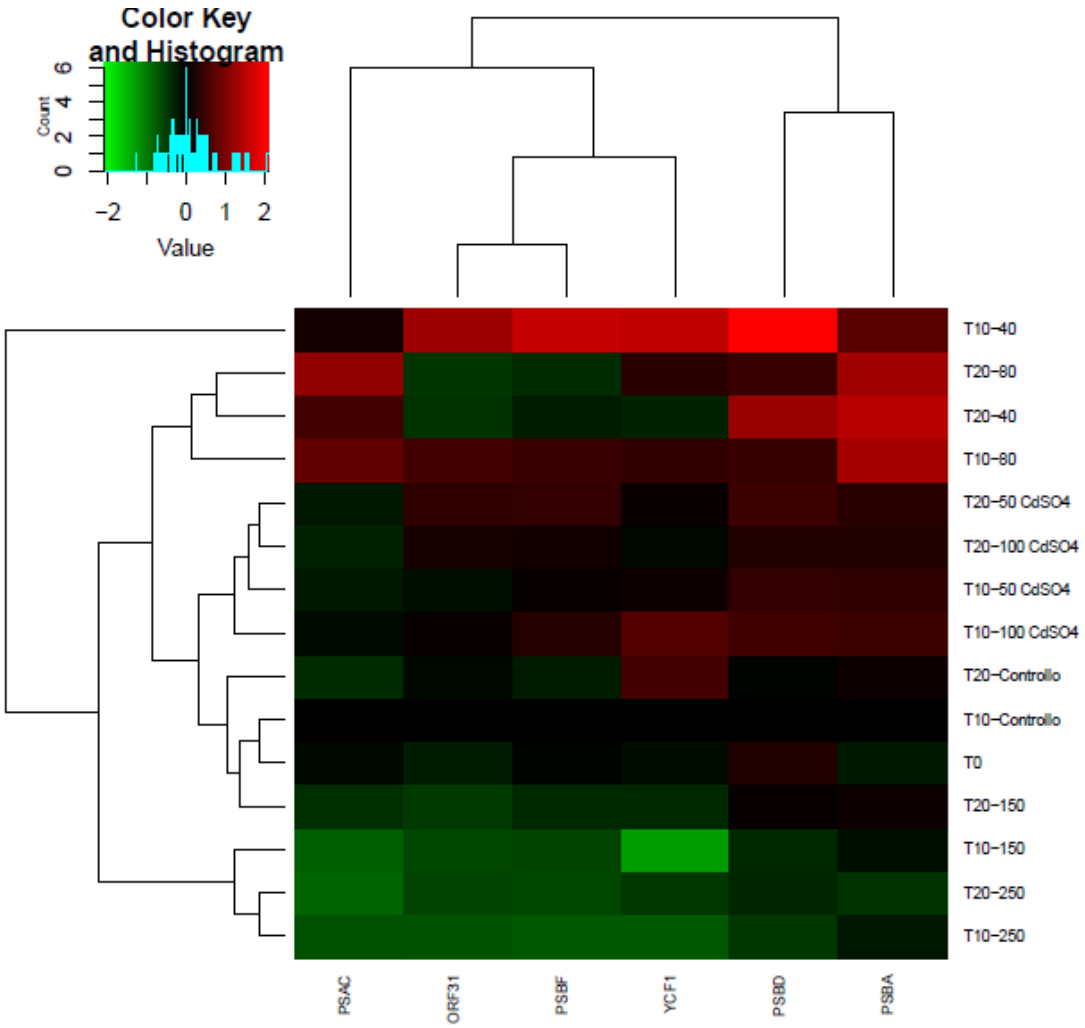

Table 4.3. Numerical results of RQ, Standard Error (SE) and t-test values relative to the heatmap reported in Fig. 4.4.

	YCF1			PSBD			ORF31			PSBA			PSAC			PSBF		
	RQ	SE	t-test	RQ	SE	t-test	RQ	SE	t-test	RQ	SE	t-test	RQ	SE	t-test	RQ	SE	t-test
T10-40	1,56	0,86	0,02	2,10	1,01	0,01	1,29	0,40	0,01	0,72	1,15	0,09	0,18	1,17	0,57	1,61	0,39	0,01
T20-80	0,33	0,77	0,08	0,47	0,52	0,02	-0,43	0,59	0,10	1,32	0,41	0,01	1,18	0,40	0,01	-0,35	0,13	0,29
T20-40	-0,28	0,50	0,14	1,26	0,36	0,00	-0,42	0,37	0,03	1,50	1,16	0,01	0,55	0,51	0,06	-0,24	0,46	0,22
T10-80	0,39	0,83	0,21	0,45	1,05	0,21	0,57	1,35	0,55	1,35	1,29	0,01	0,80	0,88	0,11	0,46	0,62	0,18
T20-50 $CdSO_4$	0,07	1,05	0,82	0,50	0,38	0,03	0,39	0,14	0,87	0,34	0,20	0,17	-0,19	0,27	0,05	0,42	0,17	0,61
T20-100 $CdSO_4$	-0,06	0,43	0,78	0,28	0,36	0,07	0,20	0,65	0,20	0,28	0,49	0,23	-0,29	0,70	0,16	0,16	0,59	0,19
T10-50 $CdSO_4$	0,11	0,67	0,48	0,42	0,52	0,02	-0,12	0,36	0,51	0,39	0,46	0,14	-0,21	0,47	0,19	0,06	0,37	0,68
T10-100 $CdSO_4$	0,68	0,50	0,02	0,54	0,58	0,02	0,07	0,18	0,08	0,51	0,57	0,07	-0,09	0,54	0,35	0,30	0,41	0,76
T20-Control	0,57	0,67	0,01	-0,04	0,49	0,70	-0,07	0,62	0,09	0,11	0,52	0,60	-0,35	0,67	0,14	-0,22	0,07	0,09
T10-Control	0,00	0,17	1,00	0,00	0,36	1,00	0,00	0,33	1,00	0,00	0,79	1,00	0,00	0,20	1,00	0,00	0,64	1,00
T0	-0,10	0,56	0,23	0,27	0,91	0,22	-0,23	0,48	0,04	-0,21	1,49	0,74	-0,08	1,21	0,79	-0,04	0,52	0,30
T20-150	-0,34	1,23	0,35	0,05	1,07	0,86	-0,48	0,29	0,04	0,11	1,44	0,71	-0,39	1,55	0,29	-0,33	0,03	0,17
T10-150	-1,29	0,60	0,01	-0,34	0,70	0,05	-0,58	0,42	0,09	-0,13	0,54	0,55	-0,78	0,57	0,01	-0,57	0,73	0,31
T20-250	-0,47	0,60	0,01	-0,32	0,73	0,27	-0,55	0,21	0,07	-0,43	0,91	0,14	-0,83	0,81	0,02	-0,59	0,27	0,13
T10-250	-0,72	0,76	0,04	-0,45	0,61	0,02	-0,68	0,59	0,51	-0,19	0,11	0,37	-0,67	0,11	0,00	-0,73	0,47	0,54

In Fig. 4.5. the heatmap shows the relative number of copies, of mitochondrial genes, for each treatment, while in Tab 4.4. relative significance levels are listed. This heatmap shows how, for both genes *COB* and *COX*, the highest $CdSO_4$ salts treatment induces significant increases of relative numbers of copies (T10-50 $CdSO_4$, T10-100 $CdSO_4$, T20-50 $CdSO_4$, and T20-100 $CdSO_4$). In particular, *COB* seems to respond strongly to higher concentrations of $CdSO_4$ salt at every exposure time. Considering these results, both *COB* and *COX* seem to be more sensible to acute effects induced by $CdSO_4$ stress and their responses permitted to distinguish clearly the differences between CdS QDs and $CdSO_4$ effects on mitochondrion.

This phenomenon could probably be induced by the toxic effect of Cd^{2+} ions on the mitochondrion biological activity.

Both chloroplast and mitochondrion could respond to the genotoxic effect, or to a genetic damage, increasing the number of some specific genes copies as a compensation mechanism. Similar effect in differences between RQ has been already observed in *A. thaliana* chloroplast exposed to an oxidative stress induced by NaCl exposition (Štefanic *et al*., 2013), and could be probably due to adaptive amplification mechanism already observed in different organism's groups (Hastings *et al*., 2000). It's also interesting to

notice how, this hypothesis, could be validated by the positions of genes that show a coherent response. In fact, both *YCF1* and *PSAC* are present in the same Cp DNA region (SSC, Fig. 3.5.), while *PSBD* and *PSBA* are both present in another Cp DNA region (LSC, Fig. 3.5.). This phenomenon could be due to different behaviour of the chloroplastic genome to stress (Hastings *et al.*, 2000).

Figure 4.5. Heatmap of mitochondrial genes relative number of copies (normalized on T10-C), for each Cd based treatment.

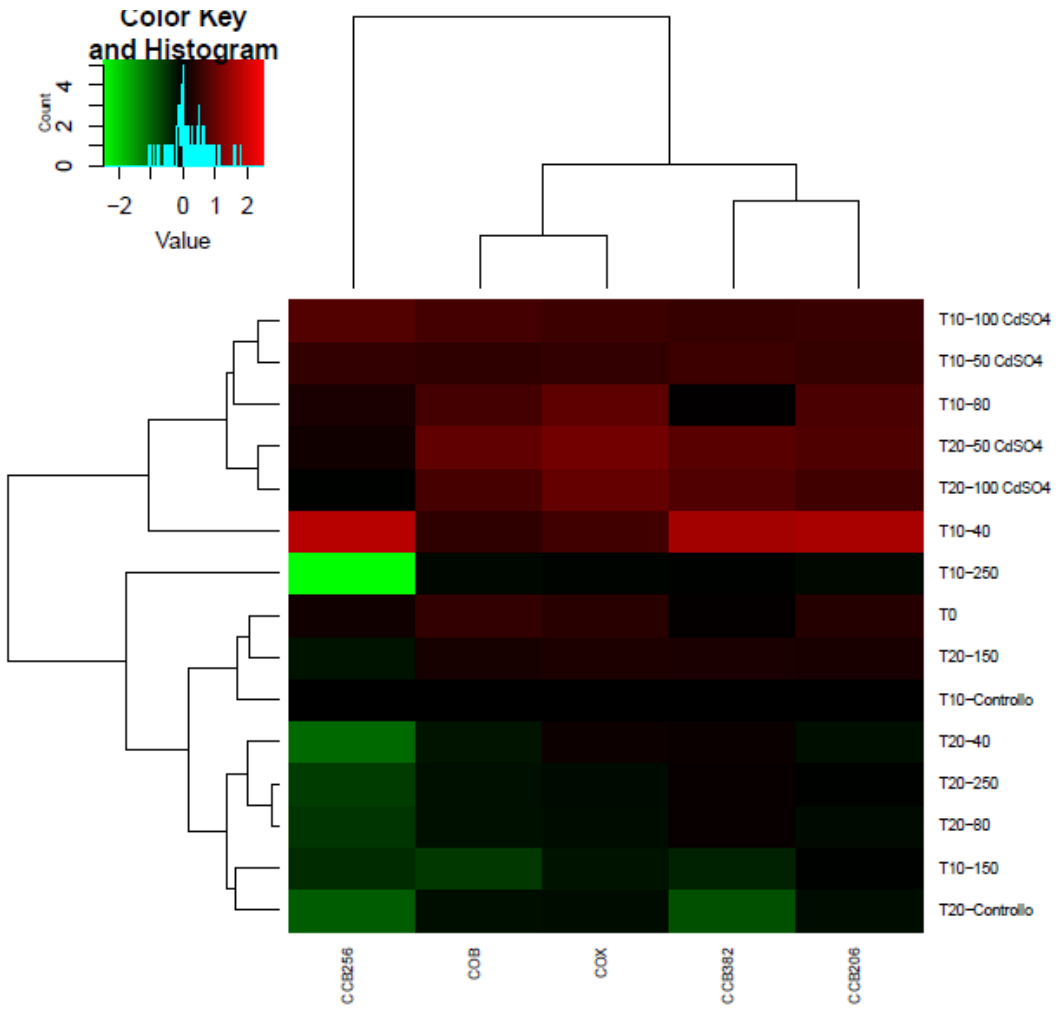

Table 4.4. Numerical results of RQ, Standard Errors (SE) and t-test (t-test) values relative to the heatmap reported in Fig. 4.5.

	COB			COX			CCB206			CCB382			CCB256		
	RQ	SE	t-test	RQ	SE	t-test	RQ	SE	t-test	RQ	SE	t-test	RQ	SE	t-test
T10-100 $CdSO_4$	0,665	0,52	0,02	0,597	0,59	0,03	0,6	0,42	0,26	0,532	0,21	0,60	0,8	0,65	0,10
T10-50 $CdSO_4$	0,451	0,21	0,00	0,501	0,21	0,00	0,5	0,38	0,05	0,601	0,52	0,16	0,496	0,17	0,23
T10-80	0,663	1,31	0,11	0,924	1,23	0,08	0,7	0,75	0,79	0,022	2,41	0,21	0,255	0,72	0,61
T20-50 $CdSO_4$	0,95	0,26	0,00	1,123	1,17	0,03	0,8	0,31	0,06	0,875	0,09	0,19	0,16	0,91	0,66
T20-100 $CdSO_4$	0,696	0,47	0,01	0,976	0,85	0,03	0,6	0,61	0,34	0,796	0,66	0,35	-0,03	0,25	0,93
T10-40	0,461	1,20	0,14	0,634	1,20	0,11	1,6	0,37	0,01	1,587	0,48	0,07	1,776	1,08	0,01
T10-250	-0,076	0,19	0,40	-0,053	0,10	0,22	-0,1	0,48	0,03	-0,03	0,22	0,17	-2,493	3,48	0,36
T0	0,488	1,18	0,20	0,399	1,23	0,16	0,4	0,33	0,27	0,04	1,00	0,71	0,174	0,88	0,68
T20-150	0,221	1,57	0,47	0,282	1,57	0,41	0,2	0,16	0,18	0,257	0,11	0,44	-0,183	0,99	0,63
T10-Control	0	0,17	1,00	0	0,31	1,00	0	0,67	1,00	0	0,66	1,00	0	1,12	1,00
T20-40	-0,207	0,09	0,02	0,124	0,43	0,32	-0,2	0,09	0,28	0,107	0,14	0,81	-1,037	2,54	0,48
T20-250	-0,171	0,85	0,97	-0,105	0,30	0,06	-0	0,20	0,24	0,081	0,09	0,38	-0,599	0,69	0,29
T20-80	-0,173	0,46	0,14	-0,121	0,29	0,43	-0,1	0,06	0,85	0,081	0,14	0,54	-0,516	1,80	0,56
T10-150	-0,547	2,77	0,30	-0,178	0,46	0,08	-0	0,78	0,24	-0,35	1,58	0,91	-0,411	0,37	0,31
T20-Control	-0,152	0,51	0,52	-0,118	0,66	0,43	-0,1	0,52	0,18	-0,79	3,06	0,19	-0,898	0,49	0,07

4.2.3. Real Time qPCR Results on Chloroplastic and Mitochondrial Genes Expression

To highlight a possible conformity between genes relative abundances and their expression levels in similar conditions, data from previous publication (Marmiroli *et al*., 2014) was compared with the present data. T20-80 CdS QDs and T20-250 CdS presented in §4.1.2. (here called T20-80 qPCR DNA and T20-250 qPCR DNA respectively) relative abundance data were compared with T20-80 CdS QDs expression for each gene (T20-80 qPCR RNA). The reference gene is rRNA 16S (standard errors of Ct are reported in Tab. 4.6.).

Moreover, T20-80 Array data (collected from Marmiroli *et al*., 2014) were included in the analysis to confirm the reliability of T20-80 qPCR RNA original data.

We can observe in Fig. 4.6. (while numerical data of RT-qPCR are reported in Tab. 4.5.) that RNA data for chloroplastic genes are in agreement with each other and in

particular, original results are in conformity with T20-80 Array results, confirming the reliability of transcriptomic data. Nevertheless, *t* test performed did not highlight significant differences except for *PSBA* and *PSAC* in T20-80 qPCR DNA.

Figure 4.6. Heatmap of chloroplastic genes relative number of copies (normalized on T10-C) for T20-80 and T20-250, T20-80 Array (Marmiroli *et al.*, 2014) and expression level T20-80 qPCR RNA.

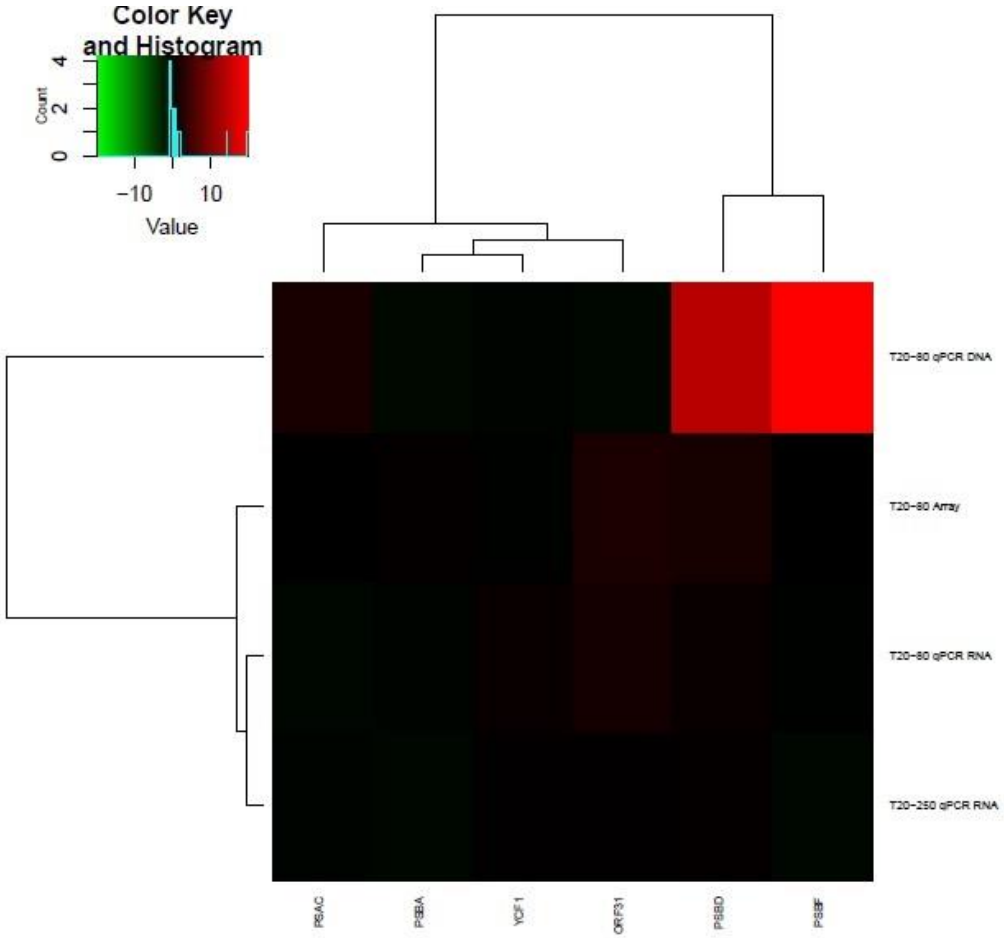

Table 4.5. Numerical data relative to the heatmap in Fig. 4.6. * Data from Marmiroli *et al.*, 2014.

	PSAC			PSBA			YCF1			ORF31			PSBD			PSBF		
	RQ	SE	t-test	RQ	SE	t-test	RQ	SE	t-test	RQ	SE	t-test	RQ	SE	t-test	RQ	SE	t-test
T20-80 qPCR DNA	1,92	0,26	0,46	-0,64	0,05	0,65	-0,44	0,20	0,08	-0,54	0,17	0,11	14,14	0,18	0,85	19,82	11,70	0,56
T20-80 array*	0,00	-	-	0,35	-	-	-0,27	-	-	2,05	-	-	1,75	-	-	-0,12	-	-
T20-80 qPCR RNA*	-0,56	-	-	-0,32	-	-	0,65	-	-	1,55	-	-	0,68	--	-	-0,28	-	-
T20-250 qPCR DNA	-0,41	0,28	0,44	-0,47	0,17	0,48	0,24	0,18	0,32	0,16	0,36	0,39	0,37	0,13-	0,10	-0,48	11,71	0,84

In Fig. 4.7. (while numerical data of RT-qPCR are reported in Tab. 4.6.) are showed transcriptomic results relative to mitochondrial genes. Also here, except for *COX* in T20-250 qPCR RNA, *t* test did not permit to highlight significant results.

Figure 4.7. Heatmap of mitochondrial genes relative number of copies (normalized on T10-C) for T20-80 and T20-250, T20-80 Array (Marmiroli *et al.*, 2014) and expression level T20-80 qPCR RNA.

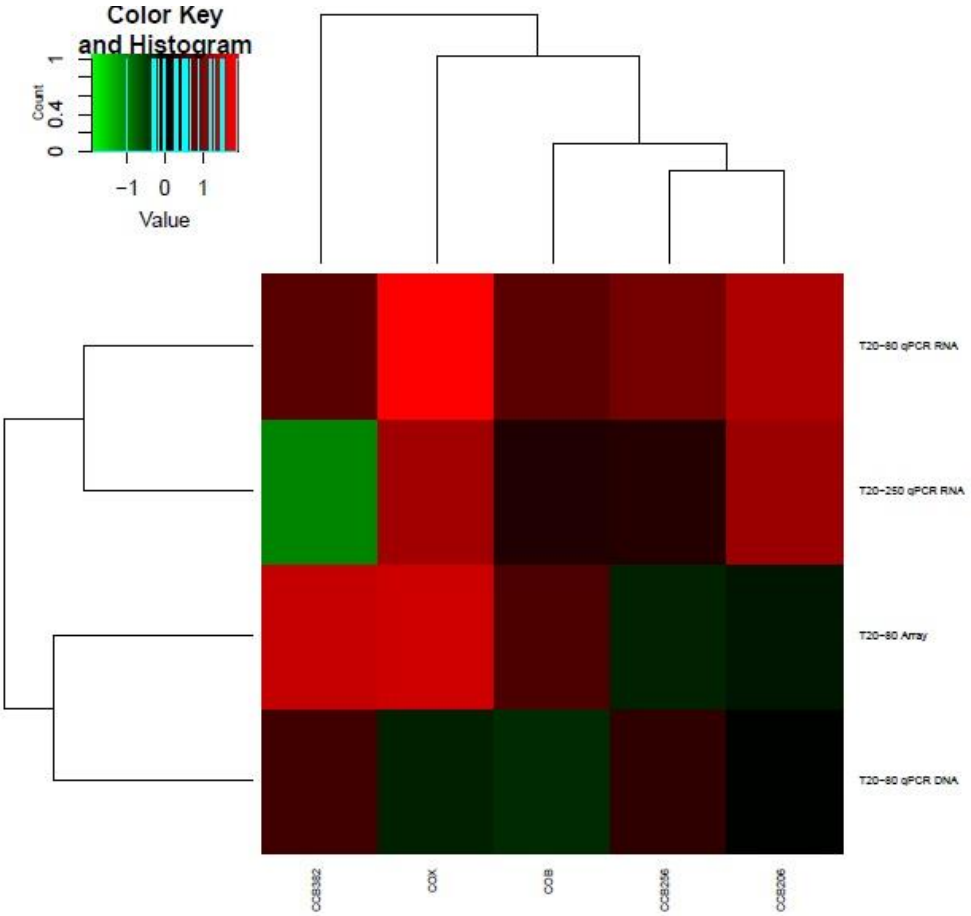

Table 4.6. Numerical data relative to the heatmap in Fig. 4.7. * Data from Marmiroli *et al.*, 2014.

	CCB382			COB			COX			CCB256			CCB206			16S
	RQ	SE	t-test	RQ	SE	t-test	RQ	SE	t-test	RQ	SE	t-test	RQ	SE	t-test	SE
T20-80 qPCR RNA*	0,68	-	-	0,68	-	-	1,94	-	-	0,88	-	-	1,31	-	-	
T20-250 qPCR DNA	-0,51	0,24	0,80	0,26	0,12	0,88	1,22	0,46	0,03	0,27	3,23	0,44	1,18	0,32	0,53	0,27
T20-80 array *	1,49	-	-	0,59	-	-	1,55	-	-	-0,27	-	-	-0,17	-	-	
T20-80 qPCR DNA	0,49	0,22	0,16	-0,33	0,13	0,06	-0,24	0,49	0,11	0,35	3,23	0,31	-0,02	0,51	0,19	0,21

The interpretation of the collected transcriptomic data in comparison with the relative abundances results is not simple. Transcriptomic data are in agreement with each other, but often not with relative abundances data.

At this level of investigation and waiting for further progresses in ENM studies, it is possible only hypotize the presence of compensation mechanism at molecular level that could lead genes to growth in number of copies to compensate lower transcription levels, and *vice versa*.

4.3. Ce, Fe, AND Zn ENM RESULTS

For each ENM and salt, an arbitrary concentration was chosen on the base of previous repeated toxicity tests.

These tests were performed to identify the (MIC), or the lowest concentrations causing the death, at least of the 50%, of exposed plants to each ENM and salt.

Tested concentrations are chosen on the base of MIC (1/2 MIC, §3.2.), they are shown in Tab. 4.4.

Table 4.4. In this table are listed, for every chemical compound in the second experiment, the tested concentration.

Chemical Compound	**Tested Concentration (mg/L) corresponding to ½ MIC**
CeO_2 NM	500
$CeCl_3$	175
Fe_2O_3 NM	500
Fe_3O_4 NM	500
$FeCl_3$	75
ZnS QDs	500
$ZnSO_4$	175

4.3.1. Physiological Parameters Results

Below are presented physiological parameters results. Physiological parameters are all presented standardized on biomass to obtain homogeneous and comparable data.

4.3.1.1. Biomass Results

Measures of biomass performed on plants exposed to different ENM and relative salts, permit to highlights some significant differences, in comparison with the control.

It can be observed in Fig. 4.8., that plants exposed to CeO_2 NPs show a significant increase in biomass production while plants exposed to $CeCl_3$ show a significant decrease in biomass. In scientific literature are already present studies that confirm how Ce based ENM could increase biomass production in different species, e.g. *P. sativum* (Zuverza-Mena *et al*., 2017).

Figure 4.8. Graphics of biomass production in plants exposed to each treatment expressed in mg. Asterisks above each histogram indicates the significance level of *t* Test.

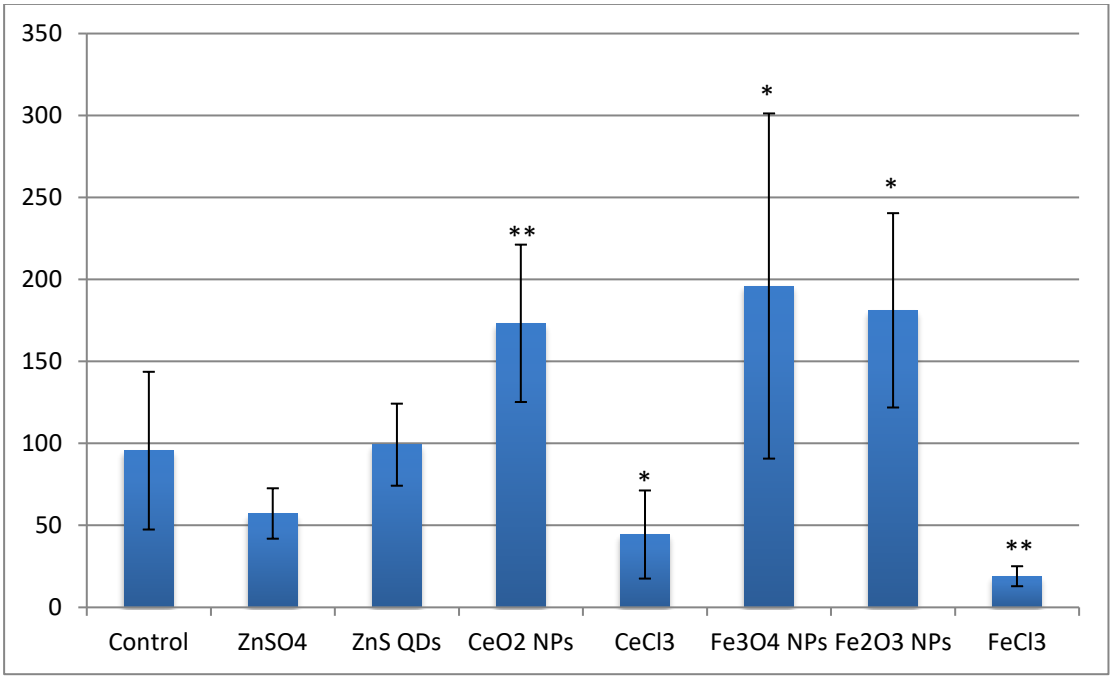

Similarly, plants exposed to both Fe_2O_3, and Fe_3O_4 ENM show a significant increase in biomass production, while plants exposed to $FeCl_3$ show a significant decrease. These results are difficult to interpret when compared with literature. In fact, Zuverza-Mena *et al*. (2017) reported how Fe based ENM generally seems to induce a deficit in plants growth by blocking water a nutrient assumption roots level. It's important to notice how plant growth media could influence the plant response to ENMs, which can explain possible differences with previous literature.

During the growth phase, plants exposed to Fe_3O_4 NPs, shows dark green colour of leaves, likely due to accumulation of Fe^{4+} ions in their tissues (Fig. 4.9.). This effect could be explained considering the relative instability of Fe based ENMs. The dissolution of Fe based ENMs is normally smaller than that of the salt, but the concentration utilized in this work, might have been higher than the one expected from environmental contamination.

Although the low dissolution rate, the instability of Fe based ENMs influenced the release of metal ions and, consequently, the response of plants to this stress.

Figure 4.9. Plants of *A. thaliana* w.t. exposed, for 20 days, to 0, 1500, 1625 1nd 1750 mg/L of Fe_3O_4 from left to right respectively. Notice how plants exposed to higher concentration shows a dark green, likely due to Fe^{4+} ions accumulation.

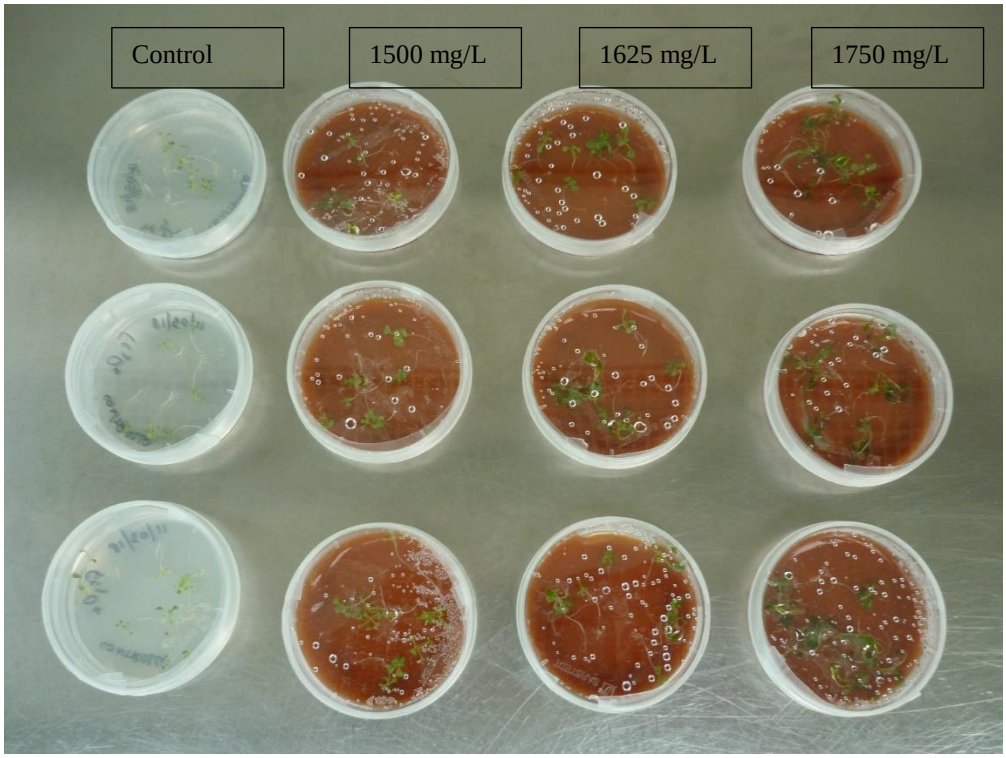

4.3.1.2. Photosynthetic Pigments Concentration Results

In Fig. 4.10. are showed results of photosynthetic pigment concentrations analyses standardized on biomass data. Although not significant, the exposure to $CeCl_3$ and $FeCl_3$ induce an increase in pigment concentration while other treatments induce a decrease. In particular, both $ZnSO_4$ and Fe_2O_3 ENM induce a significant decrease in carotenoids production.

Drawing conclusion from these results can be difficult, but for $ZnSO_4$ a possible explanation could be the damage induced by Zn based ENM Ma *et al*. (2015).

Since, Zn base ENM are relative unstable (Ma *et al*., 2015), the release of Zn^{2+} ion is similar to Zn salt; in this way a similar damage could be caused.

Table 4.5. Table relative to concentration of photosynthetic pigments, normalized on biomass quantity, for each treatment in comparison with control, chlorophyll a (Chl a), chlorophyll b (Chl b), and carotenoids. Standard Error (SE) and t-test values are reported.

	Chl a/Biomass		Chl b/Biomass		Carot./Biomass	
	t-test	SE	t-test	SE	t-test	SE
ZnSO4	0,1521	0,0033	0,4965	0,0053	0,0903	0,0020
ZnS	0,0507	0,0035	0,2398	0,0054	0,0132	0,0021
CeO2	0,9835	0,0023	0,4973	0,0054	0,7171	0,0019
CeCl3	0,4675	0,0615	0,7629	0,0052	0,3192	0,0306
Fe3O4	0,1607	0,0035	0,3319	0,0054	0,0818	0,0022
Fe2O3	0,0769	0,0036	0,2823	0,0054	0,0315	0,0022
FeCl3	0,1950	0,0436	0,2355	0,0047	0,1905	0,0823

4.3.1.3. Respiration Rate Results

The analyses of respiration rates measured in plants exposed to ENM and relative salts did not allow to evidence significant differences in comparison with the control; although an increase in respiration rate in plants exposed to $FeCl_3$ was measured (Tab. 4.6.).

Importantly, although the results are not significant, Fe bases ENM seems to induce a decrease in respiration rate while $FeCl_3$ induces an increase of the same.

On the contrary, other ENM and relative salts seem to induce a decrease of respiration rate in comparison with the control.

Table 4.6. Standard Error (SE) and t-test values relative to levels of respiration rate normalized on biomass quantity in plants exposed to each treatment.

		Chl a/Biomass			Chl b/Biomass			Carot./Biomass	
	Abs. 662 nm	**t-test**	**SE**	**Abs. 645 nm**	**t-test**	**SE**	**Abs. 470 nm**	**t-test**	**SE**
ZnSO4	0,259	0,152	0,003	0,170	0,497	0,005	0,355	0,090	0,002
ZnS	0,187	0,051	0,004	0,140	0,240	0,005	0,298	0,013	0,002
CeO2	1,680	0,984	0,002	0,613	0,497	0,005	1,897	0,717	0,002
CeCl3	1,106	0,468	0,062	0,122	0,763	0,005	1,412	0,319	0,031
Fe3O4	1,852	0,161	0,004	0,767	0,332	0,005	2,308	0,082	0,002
Fe2O3	0,449	0,077	0,004	0,256	0,282	0,005	0,687	0,032	0,002
FeCl3	1,189	0,195	0,044	0,251	0,236	0,005	2,150	0,191	0,0823

4.3.1.4. Lipid Peroxidation Results

Lipid peroxidation statistical analyses did not allow to highlight significant results. Nevertheless, it is interesting to notice that, similarly for what stated for respiration rates, Fe_2O_3 and Fe_3O_4 NPs seem to induce an opposite response in lipid peroxidation in respect to $FeCl_3$. In fact, Fe ENM induce an increase in lipid peroxidation, while $FeCl_3$ a decrease.

However, the lipid peroxidation induced by ROS produced in plants exposed to Fe based ENM was already reported by Zuverza-Mena *et al*. (2017); our results are in accordance with theirs.

Similarly, also CeO_2 NPs induce an increase in lipid peroxidation while relative Ce salts induce a decrease (Tab. 4.7.).

Table 4.7. Standard Error (SE) and t-test values of Lipid peroxidation normalized on biomass quantity data for each treatment are reported.

	MDA/Biomass		
	Abs. 532 nm	**t-test**	**SE**
ZnSO4	0,0715	0,144	0,009
ZnS	0,078667	0,252	0,011
CeO2	0,147	0,058	0,004
CeCl3	0,0585	0,128	0,012
Fe3O4	0,108	0,793	0,042
Fe2O3	0,089	0,607	0,01
FeCl3	0,031	0,081	0,012

4.3.2. RAPDs Results

RAPDs analysis performed on plant exposed for 20 d to ½ MIC of metal based ENM highlights how, in general, these compounds seem not to be genotoxic on the genomic DNA. For example, in Fig. 4.10. profiles obtained after the amplification of *OPG2* on different ENM are clearly identical to the control and similar results are obtained for all other primers selected for their profile reliability.

Figure 4.10. Profile obtained after amplification of primer OPG2 on DNA extracted from plants exposed to Ce, Fe and Zn based ENM and salts.

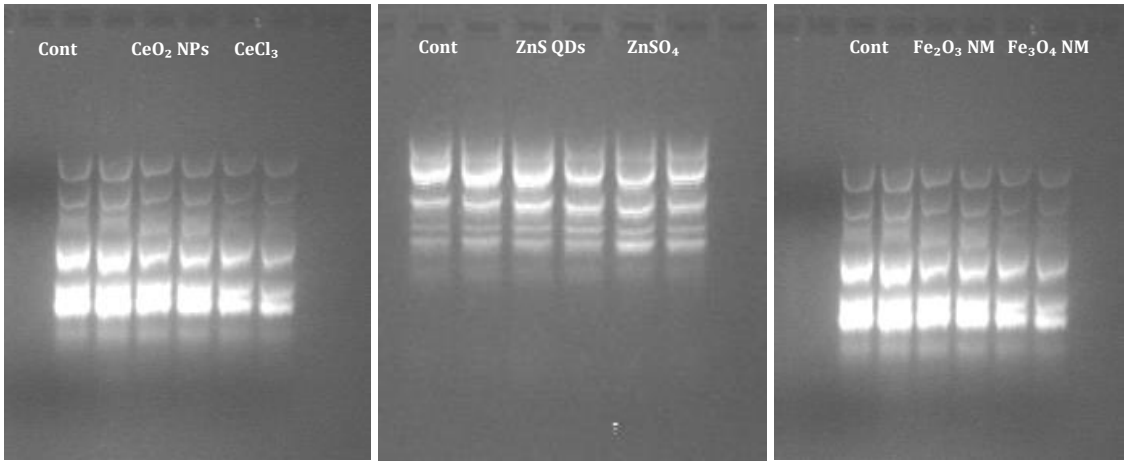

4.3.3. Real Time qPCR Results on Chloroplastic and Mitochondrial Genes Relative Number of Copies

To highlight differences in relative number of copies, in comparison with gene *16S*, of each genes Real Time qPCR were performed, as described in §3.9. starting from DNA.

In Fig. 4.11., Fig. 4.11., and Fig. 4.13. are shown the heatmaps of Ce, Fe, and Zn treatments respectively.

As reported in Fig. 4.11. (while in Tab. 4.8. relative significance levels are reported), both chloroplastic and mitochondrial genes are less abundant in relative number of copies, in comparison with the control, in plants exposed to both CeO_2 NPs and $CeCl_3$.

In particular, gene *PSBA* shows significant differences from control, while gene *ORF31* shows highly significant differences in plants exposed to CeO_2 NPs. Differences observed in two of the chloroplastic genes could be due to the effects, already observed in plants exposed to Ce based ENM, likely involved in biomass production (Fig. 4.8.).

These genes trends observed in plants exposed to Ce compounds are opposite in respect to the trends observed in other ENM, as can be observed below.

Figure 4.11. Heatmap of chloroplastic (left), and mitochondrial genes (right) relative number of copies (normalized on control), for each Ce based treatment.

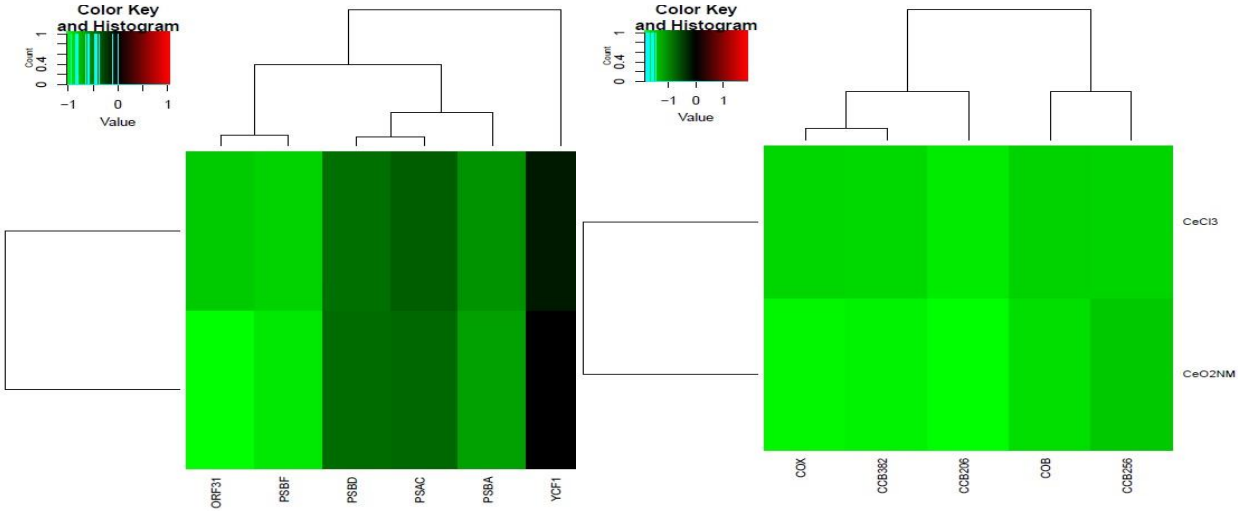

Table 4.8. Numerical values of RQ, Standard Error (SE) and t-test for both Cp and Mt genes referred to the Fig. 4.11.

	ORF31			PSBF			PSBD			PSAC			PSBA			YCF1		
	RQ	SE	t-test	RQ	SE	t-test	RQ	SE	t-test	RQ	SE	t-test	RQ	SE	t-test	RQ	SE	t-test
$CeCl_3$	-0,82	0,36	0,01	-0,851	0,39	0,08	-0,458	0,07	0,28	-0,379	0,40	0,13	-0,591	0,19	0,29	-0,107	0,37	0,18
CeO_2 NM	-1,033	0,36	0,06	-0,942	0,42	0,16	-0,436	0,39	0,27	-0,423	0,43	0,22	-0,647	0,39	0,02	0,001	0,36	0,94

	COX			CCB382			CCB256			COB			CCB206		
	RQ	SE	t-test	RQ	SE	t-test	RQ	SE	t-test	RQ	SE	t-test	RQ	SE	t-test
$CeCl_3$	-1,575	0,38	0,11	-1,591	0,32	0,71	-1,562	0,28	0,26	-1,552	0,32	0,53	-1,722	0,37	0,17
CeO_2 NM	-1,82	0,32	0,48	-1,784	0,32	0,35	-1,477	0,17	0,37	-1,641	0,44	0,81	-1,883	0,43	0,66

In Fig. 4.12. (while in Tab. 4.9. significance levels are reported) are reported results, concerning chloroplastic and mitochondrial genes, for Fe_2O_3 and Fe_3O_4 NPs and the relative salt $FeCl_3$. Generally, all genes are significative more abundant in relative number of copies in comparison with the control. Considering this behaviour, both Cp and Mt genes seem to have similar trends, responding similarly at the same stress.

The significance of the differences is very high for all $FeCl_3$ treatments, for both chloroplastic and mitochondrial genes, which confirms how the release of Fe^{3+} ions generates a stress in plant organelles.

Similarly, Fe based ENM show significant differences; these effects could probably be due to the relative instability of Fe based ENM and consequent release of Fe^{2+} and Fe^{3+} ions.

In $FeCl_3$ treatment, the release of Fe^{3+} ion is abundant; trends and statistical results observed in ENM seem to confirm the release of Fe ions in a similar way. Considering observed trends, it's possible to see how a gradient of response (in term of RQ) could be potentially traced from the more stable Fe_2O_3 NPs (lowest level of RQ), passing through more unstable Fe_3O_4 NPs, to $FeCl_3$ characterized from the highest release of metal ions (higher levels of RQ).

The general significance of the Student *t* test, for $FeCl_3$, and similarly for Fe based ENM, seem to confirm the influence of Fe ions on the growth (reflected also by low biomass production, Fig. 4.8.), on the mitochondrial activity (increase of the respiration rate Tab. 4.6., and lipid peroxidation, Tab. 4.7.) with consequent activation of compensation mechanisms at genetic level.

Figure 4.12. Heatmap of chloroplastic (left) and mitochondrial genes (right) relative number of copies (normalized on control), for each Fe based treatment.

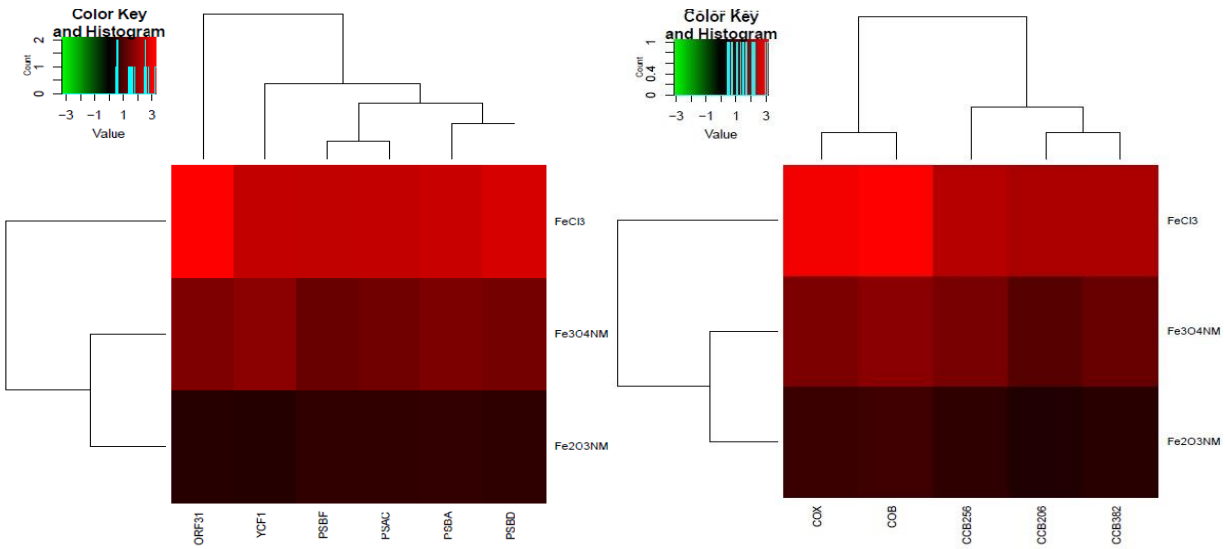

Table 4.9. Numerical values of RQ, Standard Errors (SE) and t-test for both Cp and Mt genes referred to the Fig. 4.12.

	ORF31			YCF1			PSBF			PSAC			PSBA			PSBD		
	RQ	SE	t-test	RQ	SE	t-test	RQ	SE	t-test	RQ	SE	t-test	RQ	SE	t-test	RQ	SE	t-test
$FeCl_3$	3,27	0,15	0,00	2,483	0,07	0,00	2,46	0,14	0,00	2,5	0,19	0,00	2,579	0,56	0,00	2,755	0,22	0,00
Fe_3O_4 NM	1,625	0,38	0,00	1,774	0,33	0,00	1,34	0,18	0,01	1,438	0,23	0,00	1,602	0,76	0,01	1,498	0,36	0,00
Fe_2O_3 NM	0,486	0,16	0,02	0,482	0,25	0,01	0,615	0,24	0,02	0,622	0,29	0,00	0,658	0,29	0,00	0,606	0,23	0,01

	COX			COB			CCB256			CCB206			CCB382		
	RQ	SE	t-test	RQ	SE	t-test	RQ	SE	t-test	RQ	SE	t-test	RQ	SE	t-test
$FeCl_3$	2,95	0,22	0,00	3,15	0,17	0,00	2,24	0,11	0,00	2,08	0,41	0,00	2,11	0,68	0,00
Fe_3O_4 NM	1,54	0,33	0,00	1,68	0,36	0,00	1,48	0,38	0,00	1,06	1,36	0,02	1,28	0,08	0,01
Fe_2O_3 NM	0,72	0,26	0,00	0,77	0,30	0,00	0,58	0,23	0,00	0,41	0,29	0,04	0,5	0,15	0,05

In Fig. 4.13. (while in Tab. 4.10. significance levels are reported) are graphically showed the trend, and significative levels, of chloroplastic and mitochondrial genes for ZnS QDs and $ZnSO_4$ treatments.

As observed for Fe based ENM, also Zn based ENM and Zn salt induce a general increase in relative number of copies in both chloroplastic and mitochondrial genes. Also in theis case, both Cp and mt genes seem to respond similarly to similar stresses.

The high significativity of the differences in $ZnSO_4$ are due to the release of Zn^{2+} ions causing a stress in the plant cell.

As for Fe based ENM, when compared with the relative salt show a similar behavior as ZnS QDs when compared with $ZnSO_4$. These results are likely due to the relative instability of ZnS QDs that, in solution, can release high quantity of metal ions in a similar way to the salt.

Interestingly, the significative influence of $ZnSO_4$ and ZnS QDs treatment on chloroplastic genes seems to influence the photosynthetic pigments synthesis. Althought not significatively (exept for $ZnSO_4$ effect on charotenoids). Zn treatments seem to reduce all the photosynthetic pigments concentration in comparison with the control (Tab. 4.5.).

Differently, other physiological parameters seem to reflect less obvious relations with genetic response.

Figure 4.13. Heatmap of chloroplastic (left) and mitochondrial genes (right) relative number of copies (normalized on control), for each Zn based treatment.

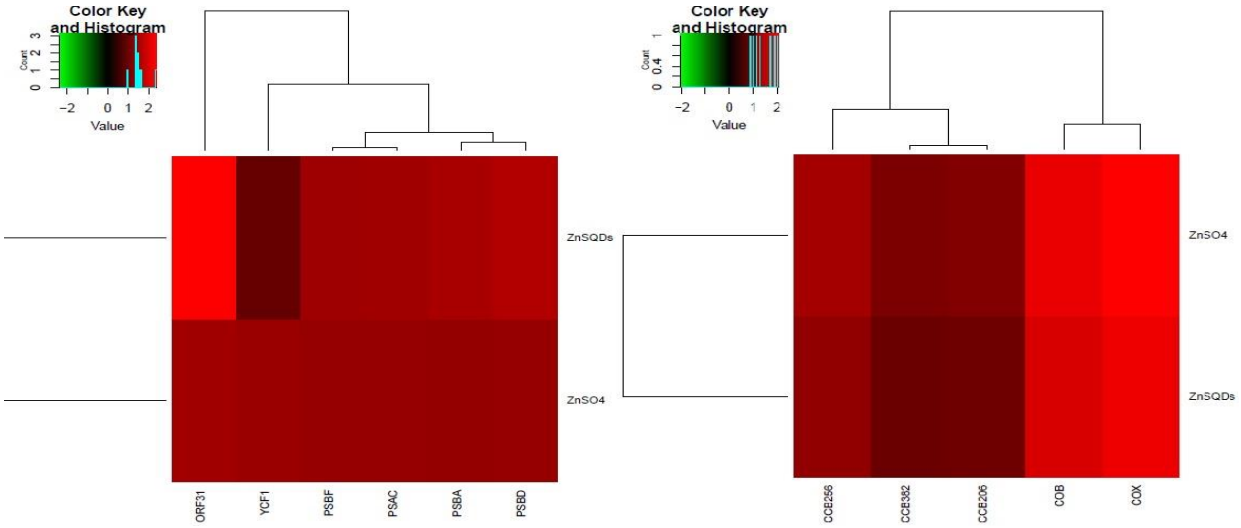

Table 4.10. Numerical values of RQ, Standard Errors (SE) and t-test for both Cp and Mt genes referred to the Fig. 4.13.

	ORF31			YCF1			PSBF			PSAC			PSBA			PSBD		
	RQ	SE	t-test	RQ	SE	t-test	RQ	SE	t-test	RQ	SE	t-test	RQ	SE	t-test	RQ	SE	t-test
ZnS QDs	2,376	0,05	0,00	0,957	1,47	0,07	1,45	0,28	0,00	1,478	0,24	0,00	1,556	0,62	0,00	1,635	0,46	0,00
$ZnSO_4$	1,472	0,08	0,00	1,429	0,11	0,00	1,386	0,24	0,00	1,387	0,12	0,00	1,356	0,62	0,00	1,387	0,04	0,00

	CCB256			CCB382			CCB206			COB			COX		
	RQ	SE	t-test	RQ	SE	t-test	RQ	SE	t-test	RQ	SE	t-test	RQ	SE	t-test
ZnS QDs	1,168	0,27	0,00	0,862	1,23	0,04	0,888	0,40	0,00	1,719	0,72	0,01	1,91	0,26	0,00
$ZnSO_4$	1,312	0,25	0,00	1,006	0,31	0,00	1,033	0,31	0,00	1,863	0,27	0,00	2,054	0,17	0,00

In Fig. 4.14. (while in Tab. 4.11. significance levels are reported) are showed trends of chloroplastic genes for all treatments. CdS QDs (T20-80) and $CdSO_4$ salt (T20-100 $CdSO_4$) are included; these two Cd treatment were chosen to allow a reliable comparison in concentrations and exposure times with other ENMs.

In this way it is possible to see the effect on chloroplastic genes of each treatment.

The heatmap highlights how treatments with more stable ENMs (CeO_2 NM, and CdS QDs) induce a similar response (decrease in relative number of copies). As stated above, $CeCl_3$ salt, despite the different charge of ions respect the ENM, induce similar response because Ce^{3+} oxidizes quickly in Ce^{4+}, once released in the environment.

Treatments with less stable ENMs (Fe_3O_4 NPs, and ZnS QDs) are similar with each other and induce similar responses: increase in relative number of copies. The corresponding salts induce similar responses likely due to the relative toxicity of high concentration of Fe^{3+} and Zn^{2+} ions.

CdS QDs show different effects on chloroplastic genes, when compared with Cd salt, likely due to their stability in respect to $CdSO_4$ and a lower tendency to release Cd^{2+} ions (data confirmed from previous study by Marmiroli *et al*., 2014).

In Fig. 4.15. (while in Tab. 4.11. significance levels are reported) are showed trends of each mitochondrial gene for each treatment. CdS QDs and $CdSO_4$ salt included.

It is possible to observe how the trends of mitochondrial genes reflect the trends already observed for chloroplastic genes. Responses of genes to more stable ENMs and relative salts are similar (decrease of relative number of copies), in the same way less stable ENMs and relative salts induce similar responses (increase of relative number of copies).

Figure 4.14. Heatmap of chloroplastic genes relative number of copies (normalized on control), for all treatments.

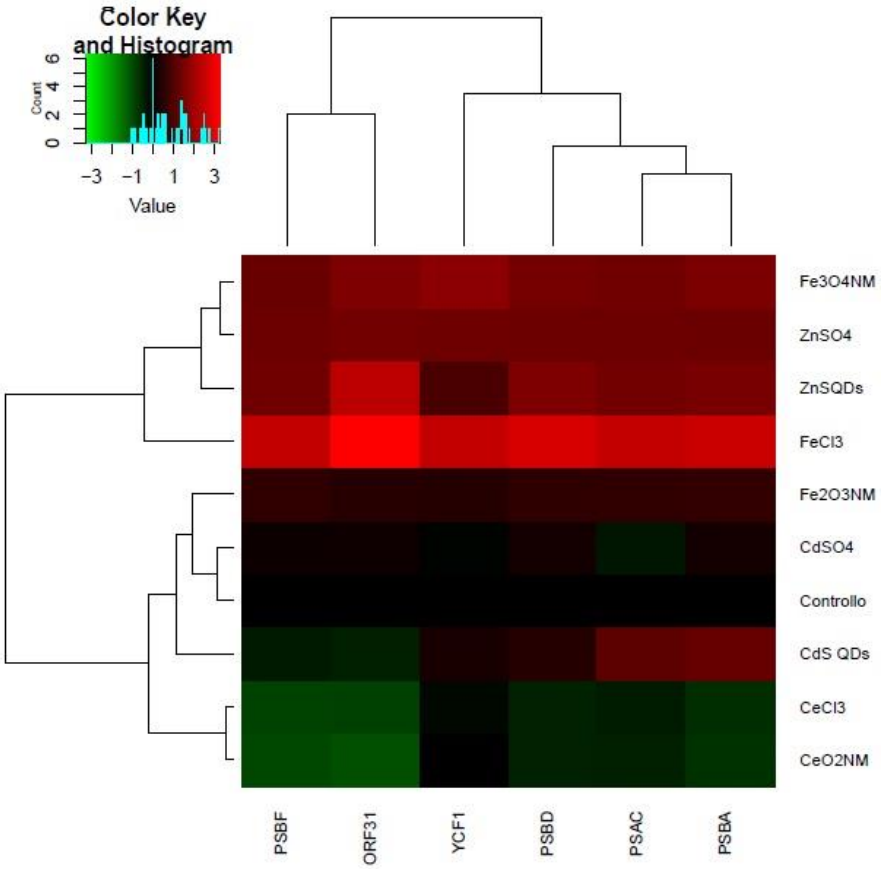

Table 4.11. Numerical values of RQ, Standard Error (ER) and t-test for Cp genes referred to the Fig. 4.14.

	PSBF			ORF31			YCF1			PSBD			PSAC			PSBA		
	RQ	SE	t-test	RQ	SE	t-test	RQ	SE	t-test	RQ	SE	t-test	RQ	SE	t-test	RQ	SE	t-test
Fe_3O_4 NM	1,34	0,18	0,01	1,625	0,38	0	1,774	0,33	0	1,498	0,36	0	1,438	0,23	0	1,602	0,76	0,01
$ZnSO_4$	1,386	0,24	0	1,472	0,08	0	1,429	0,11	0	1,387	0,04	0	1,387	0,12	0	1,356	0,62	0
ZnS QDs	1,45	0,28	0	2,376	0,05	0	0,957	1,47	0,07	1,635	0,46	0	1,478	0,24	0	1,556	0,62	0
$FeCl_3$	2,46	0,14	0	3,27	0,15	0	2,483	0,07	0	2,755	0,22	0	2,5	0,19	0	2,579	0,56	0
Fe_2O_3 NM	0,615	0,24	0,02	0,486	0,16	0,02	0,482	0,25	0,01	0,606	0,23	0,01	0,622	0,29	0	0,658	0,29	0
T20-80	-0,345	0,13	0,29	-0,432	0,59	0,1	0,329	0,77	0,08	0,465	0,02	0,52	1,18	0,4	0,01	1,319	0,41	0,01
T20-100 $CdSO_4$	0,162	0,59	0,19	0,203	0,65	0,2	-0,06	0,43	0,78	0,276	0,07	0,36	-0,294	0,7	0,16	0,277	0,49	0,23
$CeCl_3$	-0,851	0,39	0,08	-0,82	0,36	0,01	-0,107	0,37	0,18	-0,458	0,07	0,28	-0,379	0,4	0,13	-0,591	0,19	0,29
CeO_2 NM	-0,942	0,42	0,16	-1,033	0,36	0,06	0,001	0,36	0,94	-0,436	0,39	0,27	-0,423	0,43	0,22	-0,647	0,39	0,02

Figure 4.15. Heatmap of mitochondrial genes relative number of copies (normalized on control), for all treatments.

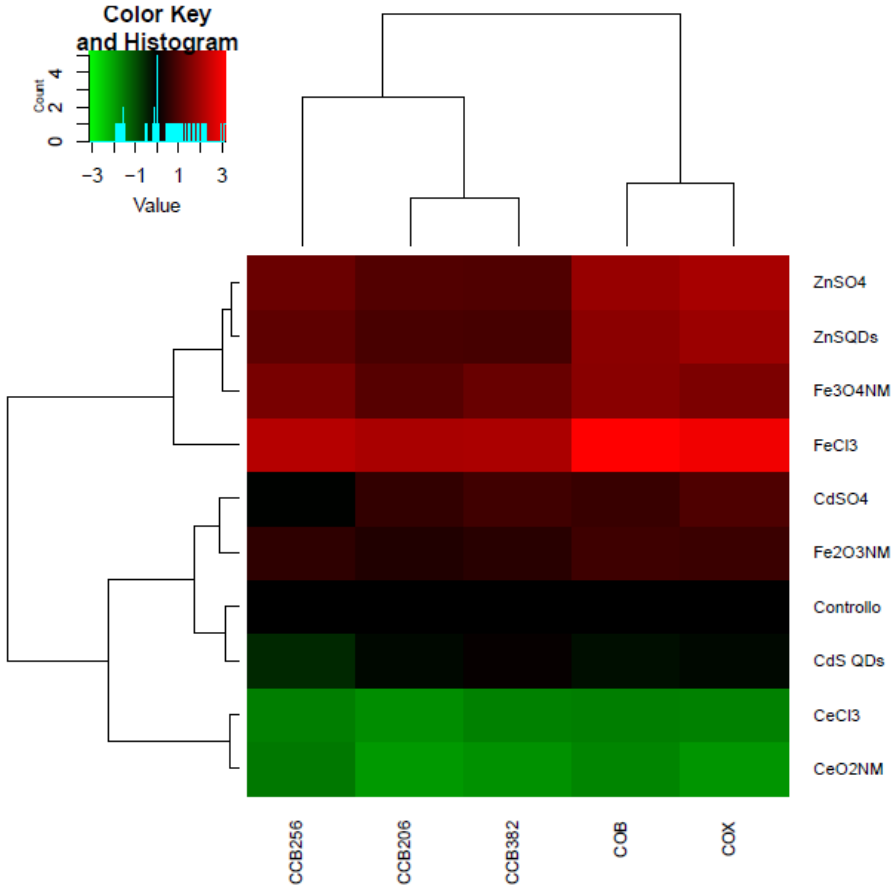

Table 4.12. Numerical values of RQ, Standard Error (ER) and t-test for Mt genes referred to the Fig. 4.15.

	CCB256			CCB206			CCB382			COB			COX		
	RQ	SE	t-test	RQ	SE	t-test	RQ	SE	t-test	RQ	SE	t-test	RQ	SE	t-test
Fe_3O_4 NM	1,48	0,38	0	1,06	1,36	0,02	1,28	0,08	0,01	1,68	0,36	0	1,54	0,33	0
$ZnSO_4$	1,312	0,25	0	1,033	0,31	0	1,006	0,31	0	1,863	0,27	0	2,054	0,17	0
ZnS QDs	1,168	0,27	0	0,888	0,4	0	0,862	1,23	0,04	1,719	0,72	0,01	1,91	0,26	0
$FeCl_3$	2,24	0,11	0	2,08	0,41	0	2,11	0,68	0	3,15	0,17	0	2,95	0,22	0
Fe_2O_3 NM	0,58	0,23	0	0,41	0,29	0,04	0,5	0,15	0,05	0,77	0,3	0	0,72	0,26	0
T20-80	-0,516	1,8	0,56	-0,1	0,06	0,85	0,081	0,14	0,54	-0,173	0,46	0,14	-0,121	0,29	0,43
T20-100 $CdSO_4$	-0,03	0,25	0,93	0,6	0,61	0,34	0,796	0,66	0,35	0,696	0,47	0,01	0,976	0,85	0,03
$CeCl_3$	-1,562	0,28	0,26	-1,722	0,37	0,17	-1,591	0,32	0,71	-1,552	0,32	0,53	-1,575	0,38	0,11
CeO_2 NM	-1,477	0,17	0,37	-1,883	0,43	0,66	-1,784	0,32	0,35	-1,641	0,44	0,81	-1,82	0,32	0,48

In conclusion, heatmaps showed in Fig. 4.14 and Fig. 4.15 highlight clearly how tested ENMs could reasonably be gathered in two groups based on relative stability. One group comprises more stable ENMs with relative salts while other group comprises less stable ENMs with relative salts.

4.3.4. Physiological Parameters and Real Time qPCR Comparison with PCA analysis

In order to highlight possible connections between physiological processes and genes relative abundances, PCA analyses were performed.

Importantly, PCA analyses constitute an integration of information already exposed in heatmaps. Therefore, PCA results are discussed considering also heatmaps results.

Chloroplastic genes relative abundances were compared with photosynthetic pigments concentrations, while mitochondrial genes relative abundances were compared with both lipid peroxidation and respiration rates data. All physiological parameters are presented standardized on biomass, in agreement with §4.2.1.

To gather in a single value the indications provided by each gene, a parameter called Molecular Response was produced summing together, for each treatment, all relative abundance values.

In Fig. 4.16. are graphically represented the PCA results obtained from photosynthetic pigments concentration and chloroplastic genes trends. Trends of photosynthetic

pigments are similar to each other and quite agree with chloroplastic genes molecular responses trends along the first principal component (PC1). This result could be reasonably due to the increasing evidences of the ENM damaging effects on photosynthetic apparatus (Hatami *et al.*, 2016). It's possible that ENM damage on photosynthetic apparatus force the plant to respond increasing the number of chloroplast and consequently the number of Cp genomes.

Moreover, on PC1, ZnS QDs clusters with their relative salt and how both Fe_2O_3 and Fe_3O_4 NPs cluster together with their relative salt.

On the second principal component, PC2, it is evident how CeO_2 NPs treatment is more similar to the control than to the corresponding salt (this behaviour it's likely due to the differences in stability). Moreover, CeO_2 NPs, that is more stable than other ENMs, have an opposite trend when compared with other ENM.

In fact, Fe and Zn based ENMs have similar trends (except for Fe_2O_3 NM that is more similar to the control than to the others, as reflected in the heatmap of Fig. 4.15.), but opposite to CeO_2 NPs trend (these results reflected what stated in §4.2.2.).

$FeCl_3$ salt shows a completely different effect on photosynthetic pigment concentration when compared with Fe based ENMs.

Figure 4.16. Graphic representation of PCA between photosynthetic pigment concentration and chloroplastic genes.

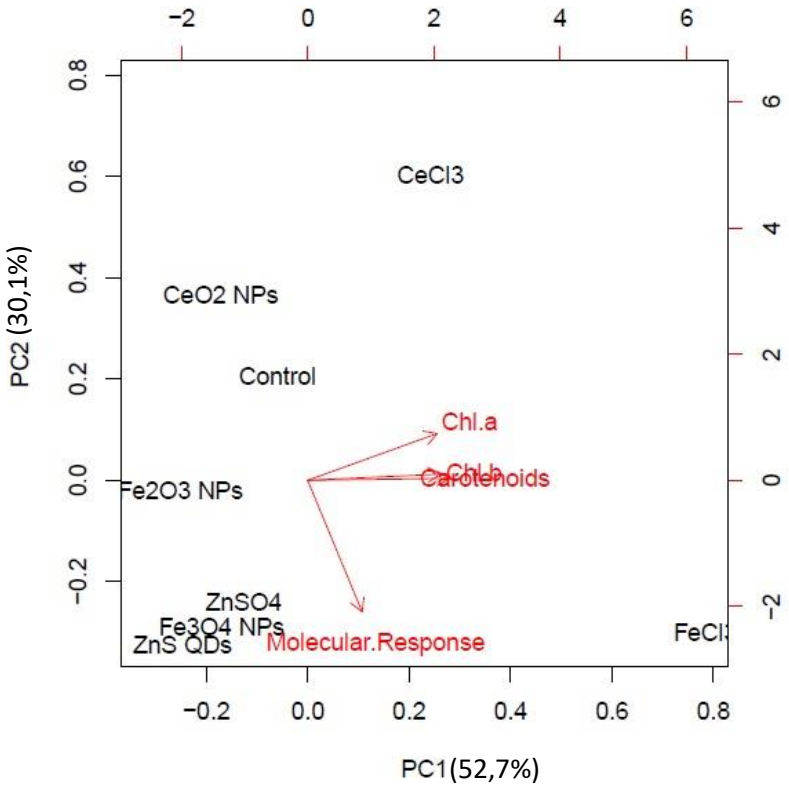

In Fig. 4.17. are graphically represented the PCA analysis between respiration rate results and mitochondrial genes trends.

This trend is similar to what observed in Fig. 4.16. On the PC1 it's also observe a similar trend of clustering ENM, in fact ZnS QDs cluster with their relative salt, while Fe based ENM cluster together and with $FeCl_3$.

Considering the PC2, trends already observed in Fig. 4.18. are similar also in Fig. 4.19. In fact, more stable CeO_2 NPs are similar to control, while Fe and Zn based ENMs are grouped together in the same quadrant (similarity already observed in Fig. 4.16.), but with opposite trend in respect to CeO_2 NPs. In this case, considering the effect on respiration rate, Fe_2O_3 NPs, Fe_3O_4 NPs, and ZnS QDs have a similar trend.

The opposite effects of $FeCl_3$ salt respect Fe based ENM are reconfirmed also in this PCA analysis.

Figure 4.17. Graphic representation of PCA between respiration rates results and mitochondrial genes.

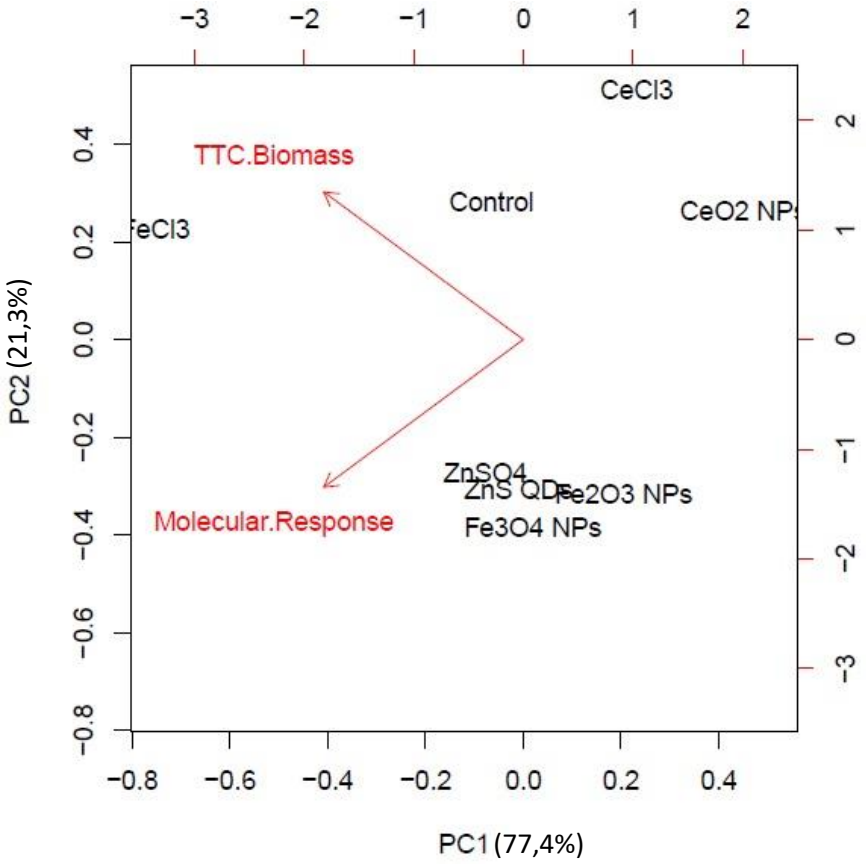

In Fig. 4.18. are graphically represented the PCA analysis between lipid peroxidation results and mitochondrial genes trends.

Interestingly, genes molecular response and lipid peroxidation show a completely opposite trend (PC1). This result is probably due to the oxidative stress caused by ROS production induced by metal based ENM (Martínez-Fernández *et al*. 2017; Soares *et al*., 2018). In fact, an increase of the ROS production could induce a damage in genetic material with a consequent decrease in RQ of Mt genes.

Moreover, on the PC2, less stable Fe and Zn based ENMs are similar to each other (as in Fig. 4.16.) and to the control when lipid peroxidation effects are considered (only Fe_3O_4 NPs show a slightly different behaviour). In this case Fe_2O_3 NPs and ZnS QDs seem to have a negligible effect on lipid peroxidation.

Instead, $CeCl_3$ salt presents a trend completely different relative to CeO_2 NPs. In fact, the latter, show an effect more similar to the control than the corresponding salt.

From the point of view of the lipid peroxidation, it seems that ZnS QDs and Fe_2O_3 ENM have more similar effects, while Fe_3O_4 ENM and CeO_2 ENM have different effects when compared each other, with other ENM and control, and with the corresponding salts.

Figure 4.20. Graphic representation of PCA between lipid peroxidation results and mitochondrial genes

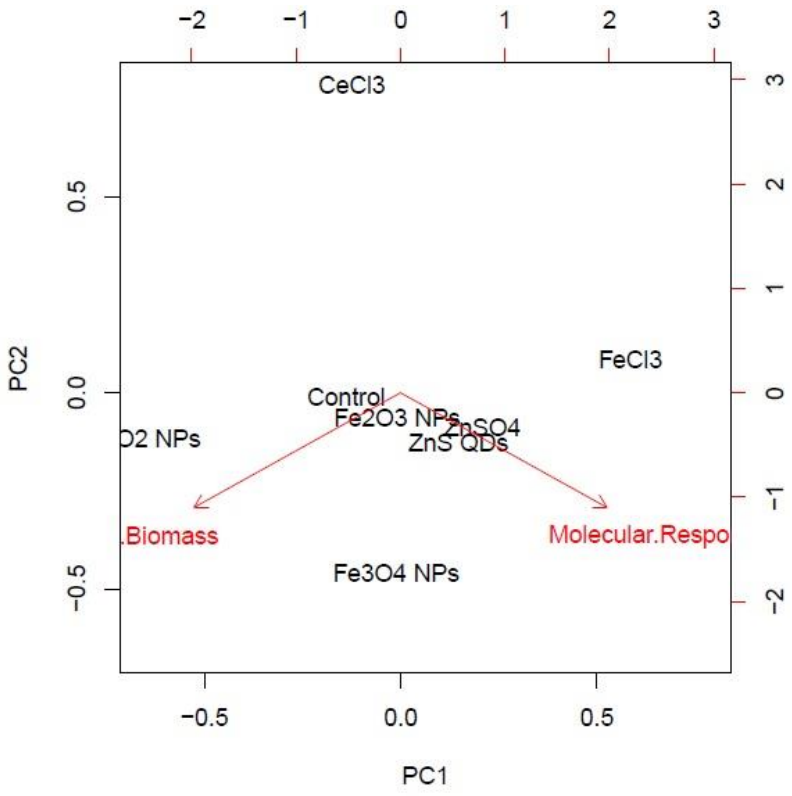

PCA analyses allowed to evidence trends between different types of parameters, and potentially find relations between variables hidden in other analyses as heatmaps.

Nevertheless, the release of metal ions could be quite consistent (§4.1.), it is clear how the less stable ENM induce similar responses in plants physiological and genetical mechanisms. More stable ENM have different effects than less stable ENM but depending on which physiological parameter it's considered (as reflected in the slightly differences between heatmaps and PCAs analyses).

The hypothesis that the potential harmful effect of ENM could be linked to the release of potential toxic metal ions, constitute the central hypothesis of this work and one of the key point of the entire research performed on ENM.

However, the role of non-metallic residual part of ENM after dissolution couldn't be ignored and potential biological effects of reaction sub-products should be always

considered in ENM characterization. Therefore, it might be possible that the non-metallic residual part of ENM could be responsible of some observed differences.

Currently, waiting for further experiment protocols to evaluate potential biological toxicity of NM, the most reliable approach is the confrontation between a metal based ENM and relative salt to highlight potential similarities in ions release. From the environmental point of view, these experiments must be carried on using realistic concentrations, in other words considering concentrations that may be actually present in the environment after an anthropic release.

5. CONCLUSIONS

Considering data collected in this work it's possible to arrive to several different conclusions. Using different tools such as RAPDs, Cp, and Mt genomes it's possible to detect effects of DNA mutation and reorganization, considering their variation in amplification profiles and in RQs, respectively. In this way they could be considered as potential biomarkers of ENM exposure/effects on model plant *A. thaliana*. The use of RAPDs permits to highlight more general presence of mutation occurring as consequence of a stress (especially on genomic DNA). The use of Cp and Mt DNA as biomarkers is supported by the fact that these two organelles (and their respectively genomes) are exposed to several dynamic processes during plant life. These continuous stresses during plant evolution has made chloroplast and mitochondrion very sensitive in responding to environmental influences (Johnson, 2019).

Moreover, differences in ENMs physico-chemical properties are reflected in differences in biomarkers responses. In fact, depending on ENMs type, responses can regard different DNA regions (as seen for Cp, and Mt genes in plants exposed to CdS QDs, and $CdSO_4$); this phenomenon has been already observed in *A. thaliana* (Štefanic *et al*., 2013), confirming the reliability of this specie for this kind of study. In other cases, responses can regard the entire genome (as seen for general, and coherent responses of Cp, and Mt genes to other metal based ENMs).

It's possible to use RQs as parameter to quantify differences between ENMs and relative salts effects, permitting to deduce general information about their stability. In general, when the ENM is unstable, its chemical behaviour is similar to the relative salt, while for more stable ENMs the behaviour could be completely different from the relative salt.

However, the response of *A. thaliana* to ENMs could be specie-specific and not general. Differences in genetic damages induces by the same ENM in different plants (see references in Tab 1.1.) could be surely reflected on Cp and Mt responses, but since the structure and function of these organelles are generally preserved in different plant species, in which similar responses could be recognized (as already observed for *ORF31* responses in Pagano *et al*., 2016, and Pagano *et al*., 2017).

It’s possible to provide useful information for future safe design of ENMs, for example in agricultural sector, preferring more stable nanoforms rather the unstable salt forms with consequent potential beneficial effects for agricultural productions, consumers and environmental health.

In addition, the construction of a database in order to collect molecular data and biological responses of different plants species for different types of ENMs from different studies could be envisaged. Such database could simplify the creation of toxicity models (*e.g.* QSAR) and meta-analysis providing a useful tool for future risk assessments.

The need of a shared protocol between ENMs toxicity researchers and a realistic forecasting of behaviour ENMs in the environment remain two of the most important problems in this field (Gardea-Torresdey *et al*., 2014; Reddy *et al*., 2016; Oomen *et al*., 2017).

6. AKNOWLEDGMENTS

In writings this work I would like to thanks Prof. Nelson Marmiroli, Prof. Marta Marmiroli, Prof. Roberta Ruotolo, Dr. Caterina Agrimonti, Dr. Luca Pagano and all the colleagues of the Dept. of Chemistry, Life Sciences and Environmental Sustainability and Dr. Andrea Zappettini and Dr. Marco Villani of IMEM-CNR, Parma, for providing some of the tested ENM.

7. REFERENCES

Atha D. H., Wamg H., Petersen E. J., Cleveland D., Holbrook R. D., Jaruga P., Dizdaroglu M., Xing B., Nelson B. C. (2012). *Copper oxide nanoparticle mediated DNA damage in terrestrial plants model*. Environ. Sci. Technol. 46(3), 1819-1827.

Atienza F. A., Jha A. N. (2012). *The Random Amplified polymorphic DNA (RAPD) Assay and Related Techniques Applied to Genotoxicity and Carcinogenesis Studies: A Critical Review*. Mutation Research 613, 76-102.

Aras S., Aydin S. S., Körpe D. A., Dönmez Ç. (2012). *Comparative Genotoxicity Analysis of Heavy Metal Contamination in Higher Plants*. Ecotoxicology. Dr. Begum G. (Ed.).

Arya M., Shergill I. S., Williamson M., Gommersall L., Arya N., Patel H. R. H. (2005). *Basic Principles of Real-Time Quantitative PCR*. Expert Rev. Mol. Diagn. 5(2), 209-219.

Becaro A. A., Siqueira M. C., Puti F. C., Regina de Moura M., Correa D. S., Marconcini J. M., Mattoso L. H. C., Ferreira M. C. (2017). *Cytotoxic and genotoxic effects of silver nanoparticles/carboxymethyl cellulose on* Allium cepa. Environ. Monit. Assess. 189:325.

Burello E., Worth A. P. (2011). *QSAR modelling of nanomaterials*. Wiley Interdiscip Rev Nanomed Nanobiothech 3(3) 298-306.

Burello E. (2017). *Review of (Q)SAR models for regulatory assessment of nanomaterials risk*. NanoImpact 8, 48-58.

Çekiç F. Ö., Ekinci S., İnal M. S., Ünal D. (2017). *Silver nanoparticles induces genotoxicity and oxidative stress in tomato plants.* Turkish Journal of Biology.

Cincu E. (2014). *Regulation of mitochondrial gene copy number in plants and the influence of impaired chloroplast function on mitochondrial motility*. PhD Thesis.

Cloutier S., Landry B. S. (1994). *Molecular Markers Applied to Plant Tissue Culture*. In Vitro Cell. Dev. Biol. 30P:32-39.

Conte C., Mutti I., Puglisi P., Ferrarini A., Regina G., Maestri E., Marmiroli N. (1998). *DNA Fingerprinting Analysis by a PCR Based Method for Monitoring the Genotoxic Effects of Heavy Metals Pollution*. Chemosphere 37, 2739-2749.

Cox A., Venkatachalam P., Sahi S., Sharma N. (2016). *Silver and titanium dioxide nanoparticle toxicity in plants: A review of current research*. Plant Physiology and Biochemistry 107, 147-163.

De la Rosa G., Garcia-Castaneda C., Vazquez-Nunez E., Alonso-Castro A. J., Basurto-Islas G., Mendoza A., Cruz-Jimenez G., Molina C. (2017). *Physiological and biochemical response of plants to engineered NM: Implications on future design*. Plant Physiology and biochemistry 110, 226-235.

Demir E., Castranova V. (2017). *Evaluation of the potential genotoxicity of quantum dots. A review*. Scientific Pages Nanothechnol 1(1), 1-19.

Deng R., Lin D., Zhu L., Majumdar S., White J. C., Gardea-Torresdey J. L., Xing B. (2017). *Nanoparticles interaction with co-existing contaminants: joint toxicity, bioaccumulation and risk*. Nanotoxicology 11:5, 591-612.

Doak S. H., Liu Y., Chen C. (2017). *Genotoxicity and cancer*. In: *Adverse Effects of Engineered Nanomaterials*. Elsevier,

EPA (2007). *Nanotechnology White Paper*.

ec.europa.eu

echa.europa.eu

euon.echa.europa.eu

Gardea-Torresdey J. L., Rico C. M., white J. C. (2014). *Trophic transfer, transformation, and impact of engineered nanomaterials on terrestrial environment*. Environ. Sci. Technol. 48, 2526-2540.

Gosh M., Jana A., Sinha S., Jothiramajayan M., Nag A., Chakraborty A., Mukherjee A., Mukherjee A. (2016). *Effects of ZnO nanoparticles in plants: cytotoxicity, genotoxicity, deregulation of antioxidant defenses, and cell-cycle arrest*. Mutation Research 807, 25-32.

Hastings P. J., Bull H. J., Klump J. R., Rosemberg S. M. (2000). *Adaptative amplification: An inducible chromosomal instability mechanism*. Cell. 103, 723-731.

Hatami M., Kariman K., Ghorbanpour M. (2016). *Engenereed nanomaterial-mediated changes in the metabolism of terrestrial plants*. Sci. Total Environ. 571, 275-291

Hellack B., Nickel C., Albrecht C., Kuhlbusch T. A. J., Boland S., Baeza-Squiband A., Wohllebend W., Schins R. P. F. (2017). *Analytical methods to assess the oxidative potential of nanoparticles: A review*. Environ. Sci. Nano 4, 1920-1934.

Hristozov D., Gottardo S., Semenzin E., Oomen A., Bos P., Peijnenburg W., van Tongeren M., Nowak B., Hunt N., Brunelli A., Scott-Fordsman J. J., Tran L., Marcomini A. (2016). *Frameworks and tools for risk assessment of manufactured nanomaterials*. Environment International. 95, 36-53.

Holden P. A., Nisbet R. M., Lenihan H. S., Miller R. J., Cherr G. N., Schimel J. P., Gardea-Torresdey J. L. (2013). *Ecological nanotoxicology: integrating nanomaterial hazard consideration across the subcellular, population, community and ecosystem levels*. Acc. Chem. Res. 46(3), 813-822.

Johnson I. G. (2019). *Tension and resolution:Dynamic, evolving populations of organelle genomes within plant cells*. Mol. Plant. 12, 764-783.

Khan M. N., Mobin M., Abbas Z. K., AlMutairi K. A., Siddiqui Z. H. (2017). *Role of nanomaterials in plants under challenging environments*. Plant Physiology and Biochemistry. 110, 194-209.

Kumari M., Mukherjee A., Chandrasekaran N. (2009). *Genotoxicity of silver nanoparticles on* Allium cepa. Science of Total Environment. 407, 5243-5246.

Lee S., Chung H., Kim S., Lee I. (2013). *The genotoxic effect of ZnO and CuO nanoparticles on early growth of buckwheat,* Fagopyrum esculentum. Water, Air and Sioli Pollution. 224:1668.

Lowry G. V., Gregory K. B., Apte S. C., Lead J. R. (2012). *Transformation of nanomaterials in the environment*. Environ. Sci. Technol. 46(13), 6893-6899.

Ma C., White J. C., Xing B., Dhankher O. P. (2015). *Phytotoxicity and Ecological Safety of Engineered Nanomaterials*. International Journal of Plant and Environment 1(1), 9-15.

Ma Y., Yao Y., Yang J., He X., Ding Y., Zhang P., Zhang J., Wang G., Xie C., Luo W., Zhang J., Zheng L., Chai Z., Zhao Y., Zhang Z. (2018). *Trophic transfer and*

transformation of CeO_2 nanoparticles along a terrestrial food chain: influence of the exposure routes. Environ. Sci. Technol. 52(14), 7921-7927.

Marmiroli M., Pagano L., Savo Sardaro M. L., Villani M., Marmiroli N. (2014). *Genome-Wide Approach in* Arabidopsis thaliana *to Assess the Toxicity of Cadmium Sulfide Quantum Dots*. Environ. Sci. Technol. 48, 5902-5909.

Marmiroli M., Mussi F., Imperiale D., Lencioni G., Marmiroli N. (2017). *Abiotic Stress Response to As and As + Si, Composite Reprogramming of Fruit Metabolites in Tomato Cultivars*. Front. Plant. Sci. 8:2201.

Marmiroli M., Mussi F., Pagano L., Imperiale D., Lencioni G., Villani M., Zappettini A., White J. C., Marmiroli N. (2020). *Cadmium sulfide quantum dots impact* Arabidopsis thaliana *physiology and morphology*. Chemosphere, 240, 124856.

Martínez-Fernández D., Vítková M., Michálková Z., Komárek M. (2017). *Engineered nanonamaterials for phytoremediation of metal/metalloid-contaminated soils: implications for plant physiology*. In: Ansari A. A., Gill S. S., Gill R., Lanza G. R., Newman L. (eds.). *Phytoremediation.* Springer, Cham.

Mattar A. Z., Sammour R. H., El-kholy Aziza S., Seada May L. (2015). *Detection of genotoxic effect of wastewater on* Vicia faba *L. using biochemical essay and RAPD markrs*. Egypt. Jou. Bot., Vol. 55, No.2, pp. 281-296.

Oomen A. G., Steinhausen K. G., Bleeker E. A. J., van Broekhuizen F., Sips A., Dekkers S., Wijnhoven S. W. P., Sayre P. G. (2017). *Risk assessment frameworks for nanomaterials: Scope, link to regulation, applicability, and outline for future directions in view of needed increase in efficiency*. Nanoimpact 9, 1-13.

Pacheco I., Buzea C. (2018). *Nanoparticles uptake by plants: Beneficial or detrimental?* In: Faisal M., Saquib Q., Alatar A. A., Al-Khedhairy A. A. (Eds.). (2018). *Phytotoxicity of nanoparticles*. Springer International Publishing AG.

Pagano L., Servin A. D., De La Torre-Roche R., Mukherjee A., Majumbdar S., Howthorne J., Marmiroli M., Maestri E., Marra R. E., Isch S. M., Dhankher O. P., White J. C., Marmiroli N. (2016). *Molecular response of crop plants to enginereed nanomaterials*. Environ. Sci. Technol. 50, 13, 7198-7207.

Pagano L., Pasquali F., Majumdar S., De La Torre-Roche R., Zuverza-Mena N., Villani M., Zappettini A., Marra R. E., Isch S. M., Marmiroli M., Maestri E., Dhankher O. P., White J. C., Marmiroli N. (2017). *Exposure of* Curcubita pepo *to binary combinations of engineered nanomaterials: physiological and molecular response*. Environmental Sci.: Nano. 4(7), 1579-1590.

Pagano L., Maestri E., White J. C., Marmiroli N., Marmiroli M. (2018). *Quantum dots exposure in plants: Minimizing the adverse response*. Current Opinion in Environmental Science and Health 6, 71-76.

Pramanik A., Datta A. K., Gupta S., Gosh B., Das D., Kumbhakar D. V. (2017). *Assessment of genotoxicity of enginereed nanoparticles (cadmium sulphide – CdS and copper oxide – CuO) using plant model (*Coriandrum sativum *L.)*. Int. J. Res. Pharm. Sci., 8(4), 741-753.

Priester J. H., Moritz S. C., Espinosa K., Ge Y., Wang Y., Nisbet R. M., Schimel J. P., Goggi A. S., Gardea-Torresdey J. L., Holden P. A. (2017). *Damage assessment for soybean cultivated in soil with either CeO_2 or ZnO manufactured nanomaterials*. Science of the Total Environment 579, 1756-1768.

Reddy P. V. L., Hernandez-Viezcas J. A., Peralta-Videa J. R., Gardea-Torresdey J. L. (2016). *Lesson learned: are engineered nanomaterials toxic to terrestrial plants?* Science of the Total Environment 578, 470-479.

Remédios C., Rosário F., Bastos V. (2012). *Environmental nanoparticles interactions with plants: morphological, physiological, and genotoxic aspects*. Journal of Botany. Article ID 751686, 8 pages.

Rizwan M., Ali S., Qayyum M. F., Ok Y. S., Adrees M., Ibrahim M., Zia-ur-Rehman M., Farid M., Abbas F. (2017). *Effect of metal and metal oxide nanoparticles on growth and physiology of globally important food crops: A critical review*. Journal of Hazardous Materials 322, 2-16.

Ruotolo R., Maestri E., Pagano L., Marmiroli M., White J. C., Marmiroli N. (2018). *Plants response to metal-containing nanomaterials: an omic-based perspective*. Environ. Sci. Technol. 52(5), 2451-2467.

Shaymurat T., Gu J., Xu C., Yang Z., Zhao Q., Liu Y., Liu Y. (2012). *Phytotoxic and genotoxic effects of ZnO nanoparticles on garlic (*Allium sativum *L.): A morphological study*. Nanotoxicology, 6, 241-248.

Selk H., Handy R. D., Fernandes T. S., Klaine s. T., Petersen E. J. (2016). *Nanomaterials in the aquatic environment: a European Union-United States perspective on the status of ecotoxicity testing, research priorities, and challenges ahead*. Environmental Toxicology and Chemistry Vol. 35, No. 5.

Silva S., Oliveira H., Silva A. M. S., Santos C. *The cytotoxic targets of anatase or rutile + anatase nanoparticles depend on the plant species*. Biologia Plantarum 61(4): 717-725.

Soares C., Pereira R., Fidalgo F. (2018). *Metal-based nanomaterials and oxidative stress in plants. Current aspects and overview*. In: Faisal m. (Ed.). *Phytotoxicity of Nanoparticles*. Sprnger International Publishing AG, Part of Springer Nature 197.

Sobieh S. S., Kheiralla Z. M. H., Rushdy A. A., Yakob N. A. N. (2016). *In vitro and in vivo genotoxicity and molecular response of silver nanoparticles on different biological model systems*. Caryologia 69, 147-161.

Štefanic P. P., Koffler T., Adler G., Bar-Zvi D. (2013). *Chloroplast of salt grown* Arabidopsis *seedling are impaired in structure, genome copy number and transcript levels*. PLoS ONE 8(12): e82548.

Tripathi D. H., Singh S., Singh S., Pandey R., Singh V. P., Sharma N. C., Prasad S. M., Dubey N. K., Chauhan D. K. (2017). *An overview of manufactured nanoparticles in plants: Uptake, translocation, accumulation and phytotoxicity*. Plant Physiology and Biochemistry 110, 2-12.

Wang H., Wu F., Meng W., White J. C., Holden P. A., Xing B. (2013). *Engineered nanoparticles may induce genotoxicity*. Environ. Sci. Tachnol. 47(23), 13212-13214.

Zhang P., Ma Y., Zhang Z (2015). *Interactions between engineered nanomaterials and plants: phytotoxicity, uptake, translocation, and biotransformation*. In: Siddiqui M., Al-Whaibi M., Mohammad F. (eds.) *Nanotechnology and Plant Sciences*. Springer, Cham.

Zuverza-Mena N., Martinez-Fernandez D., Du W., Hernandez-Viezcas J. A., Bonilla-Bird N., Lopez-Moreno M. L., Komarek M., Peralta-Videa J. R., Gardea-Torresdey J. L.

(2017). *Exposure of engineered nanomaterials to plants: Insights into the physiological and biochemical response – A review*. Plant Physiology and Biochemistry 110, 236-264.

8. SITOGRAPHY

cdn.biologydiscussion.com

efsa.europa.eu

primer3.ut.ee

researchpower2.ewha.ac.kr

string-db.org

understandingnano.com

www.arabidopsis.org

www.chemsafetypro.com

www.epa.org

www.fda.org

www.ncbi.nlm.nih.gov

www.nwlifescience.com